VARIATION OF RAINDROP CATCH DUE TO AIRFLOW DISTURBANCES AROUND A STANDARD RAINGAGE

Thesis for the Degree of Ph. D.

MICHIGAN STATE UNIVERSITY

CHARLES CARSTEN MUELLER

1969

This is to certify that the

thesis entitled

VARIATION OF RAINDROP CATCH DUE TO AIRFLOW DISTURBANCES AROUND A STANDARD RAINGAGE

presented by

Charles Carsten Mueller

has been accepted towards fulfillment
of the requirements for

Ph.D. degree in Agricultural Engineering

E H Kidder
Major professor

Date 12/18/68

O-169

ABSTRACT

VARIATION OF RAINDROP CATCH DUE TO AIRFLOW DISTURBANCES AROUND A STANDARD RAINGAGE

By

Charles Carsten Mueller

The inadequacies of rainfall measurements have been realized for many years, however the need for greater accuracy in precipitation measurements was not appreciated until cloud physics studies by radar techniques were initiated. Runoff forecasting for engineering design purposes is also requiring greater accuracy in precipitation measurement as runoff related structures' importance and cost of construction increase.

While a raingage's spatial position has an important influence on the gage's performance, the physical presence of the gage itself must be considered a hindrance to its operation. Obstruction to airflow in the vicinity of the gage, due to the gage's presence, results in disturbances in the local precipitation pattern. This study's objective was to determine the airflow pattern around a U. S. Weather Bureau Standard Raingage, to analyze the airflow's effect on drops approaching the gage's funnel and to obtain a correction curve relating percent of catch to drop size and air velocity past the gage.

Charles Carsten Mueller

The airflow pattern was determined by measurements with a three sensor hot film anemometer system in a wind tunnel using model gages. This three dimensional flow field description and the known aerodynamic drag characteristics of water drops were used in a digital computer to simulate the drops' movements as they approached the gage. The drop paths thus determined were then analyzed to establish the gage's effectiveness in measuring precipitation.

Using drop sizes of 1 to 5 millimeters in diameter, it was found that the gage caught from 103 to 11 percent of the drops as the free stream airflow velocity increased from 10 to 50 feet per second. In general, the decrease in catch was less pronounced as drop size increased.

Approved E H Kidder
Major Professor

Approved E H Kidder for C W Hall
Department Chairman

VARIATION OF RAINDROP CATCH DUE TO AIRFLOW DISTURBANCES AROUND A STANDARD RAINGAGE

By

Charles Carsten Mueller

A THESIS

Submitted to
Michigan State University
in partial fulfillment of the requirements
for the degree of

DOCTOR OF PHILOSOPHY

Department of Agricultural Engineering

1969

To Glenda

ACKNOWLEDGMENTS

The author wishes to express his appreciation and thanks to Prof. E. H. Kidder, committee chairman, Prof. M. L. Esmay, Prof. O. Andersland, Prof. R. Hamelink and the Agricultural Engineering Department, for their help and support that aided the completion of this study.

I thank you.

TABLE OF CONTENTS

LIST OF TABLES

LIST OF FIGURES

INTRODUCTION

As early as 400 BC raingages were in use. It is reported in early Indian writings, translated by Shamasastry (1915), that: "In (front of) the store houses, a bowl with its mouth as wide as an aratni (24 angulas) shall be set up as a varshamana (raingage). . . ." Typical rainfall quantities are given for various parts of the country. Rainfall predictions were also being made: "A forecast of such rainfall can be made by observing the position, motion and pregnancy of Jupiter, the raise and set motion of Venus and the natural or unnatural aspect of the sun." Just how these factors were used to form conclusions is not discussed, however, the rainfall records were used to determine what crops were to be planted.

It is now realized that the accuracy of yesterday's and today's rainfall measurements is often less than desirable and the errors are usually unpredictable. The advent of precipitation measurements and cloud physics studies by radar techniques has pointed this out. However, the inadequacies of raingages in general have been realized for at least 200 years. Heberden (1769) found that similar gages at different heights caught different amounts of rainfall. Many investigators since that time have shown that gage catch tends to decrease as wind velocity increases. This is especially true during periods of snowfall.

The precipitation gage is one of the primary instruments of observation in meteorology, hydrology and climatology. As a tool for climatological data collection the present day raingages have been considered adequate. However, for engineering purposes, such as runnoff forecasting necessary for design work, and for radar and cloud physics studies, today's gage is often inadequate.

While gage exposure plays an important role in the instrument's performance, the gage itself must be considered as a hinderance to accurate measurements due to its own obstruction to airflow in the immediate vicinity of the gage and the resulting disturbance in the local precipitation pattern. This research report concerns itself with the measurement of the disturbed airflow pattern around a gage and evaluating the resulting error on the gage's catch. While the techniques used are time consuming, they are applicable to the evaluation of new or modified gages.

The objective of this study was to obtain a correction curve for use with a U. S. Weather Bureau Standard Raingage relating percent of catch to drop size and air velocity past the gage.

LITERATURE REVIEW

Gage Errors

Several sources of errors are present in most rain-gages and gage installations. Kurtyka (1953) has estimated these errors as being:

TABLE 1.--Approximate errors in precipitation measurements.

	% error
evaporation	-1.0
adhesion	- .5
color	- .5
inclination	- .5
splash	+1.0
exposure	-5.0 to -80.0

Evaporation losses varied with gage and air temperature. Horton (1919) showed that about 70 percent of the evaporative losses occurred during the 12 hour night period. He also found that the water loss due to evaporation over a 7 day period (at 70° F) was equivalent to .01 inch of rain. Painting of gage funnels is not desirable due to the varying effects of aging paint. Differences in gage losses due to gage color have been found to be on the order of one percent, Wild (1873), with a white gage indicating about one percent more than a black gage.

Due to most raingage designs, the gage is more apt to receive splash from the surrounding area than to lose it. Gold (1931) found that with a wet surface, drops 2 mm in diameter could create splash up to 4 feet high. The errors due to splash are mainly additive. However, other gage errors are nearly always in a negative direction, therefore many investigators judge a gage on its ability to catch more precipitation than others.

Many experimenters have shown the effect of exposure on gage performance. Heberden (1769) conducted an experiment that showed a decrease in precipitation with height. His highest gage, 151 feet above ground level, caught 46% less than a gage at ground level. (It was postulated that electricity was concerned with this phenomenon.) A significant experiment carried out by Arnold, and reported by Symons (1871) showed that there was, in fact, no significant difference in rainfall at ground level and at an elevated station. He used two gages, one at 5 feet, the other at 30 feet, with sloping orifices that always faced into the wind. Over a 5 year period these two gages almost always caught the same amount of rain (.19 inch total difference) and were in good agreement (±0.5%) on a yearly basis.

In general the orifice height of gages used throughout the world covers a small range, from 1 foot to 6.6 feet (2 meters). Exceptions are totalizing gages in heavy snowfall areas which may reach 15 to 20 feet in height.

TABLE 2.--Comparison of various Standard Gages. From Kurtyka (1953).

Country	Type Gage	Orifice Diameter (inches)	Orifice Height (inches)
England	M. O. pattern	8	12
England	Snowdon	5	12
Australia	8-inch type	8	12
France	Tonnelot	8.88	28.3
Austria	Kostlivy	9.93	20.3
United States	U.S. Weather Bureau Standard	8	31±
France	Scientific Assoc.	8.88	39.4
China	Board	7.91	39.4
South Africa	5-inch type	5	48
Holland	DeBilt	8.88	59.1
Germany	Hellmann	6.28	59.1
Sweden	Swedish	14.06	59.1
Russia	Russian	9.93	78.8

Several conflicting reports have been made concerning the effect that orifice size has on precipitation catch. Conover's (1951) experiments with a 3/4 inch orifice gage indicated a higher catch than larger orifice gages. Through a mathematical treatment, Howell (1946) showed that a small gage should be more effective in precipitation measurements. Wild (1885) reported on tests of Calne and Stratfield-Turgis using 8 gages with from

1 to 24 inch orifices that showed there was little difference with orifices over approximately 4 inches. Smaller orifices indicated less rainfall.

No other factor in rain or snow measurement is as important as instrument exposure. A gage site and the air movement over the site area should be representative of the area that the gage readings are supposed to represent.

However, the gage itself presents an obstruction to the general airflow pattern, creating increased velocities over and around the gage, and eddies in its lee and possibly in its funnel. The increased airflow velocity over a gage may carry the smaller and lighter water drops across the gage's orifice instead of allowing them to fall into it. This loss is directly related to wind velocity. That is, as wind velocity increases the losses due to the disturbed airflow pattern increases.

Gage Shields

Several gage shields have been devised in an effort to reduce the adverse airflow pattern that exists around a gage. None have been completely successful. "The effect of windshields on raingages is to divert the flow of air down and around the gage so that there is no updraft in the region of the orifice of the gage to cause a corresponding area of minus precipitation," Kurtyka (1953).

An early form of gage shield was developed by Stevenson (1842). His gage's orifice was set at ground level and was protected from splash by a surrounding brush mat. It produced the desirable aerodynamic characteristics, and performed well with rain, but snow tended to drift into the orifice. The two best known gage shields are those developed by Alter (1937) and Nipher (1878). Several variations of these shields have also been studied.

The Nipher shield is trumpet shaped with the flared end upward and level with the gage orifice. The Alter shield has a similar shape but is formed of movable metal strips spaced in a ring around the gage. These were primarily used with storage gages in snowfall regions.

TABLE 3.--Deviation of unshielded gage catch as compared to a gage with Nipher shield. From Borstein (1884).

Wind mph	45 heavy rains Number of days	45 heavy rains deficit (%)	26 fine rains Number of days	26 fine rains deficit (%)
0 - 1			4	23
1 - 3	17	6	8	25
4 - 7	13	13	6	18
8 - 13	7	14	6	46
13 - 18	6	17	2	52

According to Bernard (1938) the Nipher shield was theoretically correct for sampling snow in windy conditions. However, it was found that the rigid horizontal shelf-like portion of the shield funnel collected snow which later blew into the gage. Screens have been used on the horizontal portions of the Nipher shield to effectively reduce splash into the gage.

Neiss (1961) studied the variation of snow catch with shielded and unshielded gages with 4 pairs of gages in Michigan. While differences were small during warm months, the mean ratio of unshielded gage to shielded gage snow catch varied from about .9 to .5 as the average wind speed increased from 2 to 14 mph.

Warnick (1956) has made extensive studies using a specially constructed wind tunnel, sawdust snow and various photographic techniques to evaluate the effectiveness of several types of gages and shields to measure snowfall. The following table is indicative of Warnick's results.

TABLE 4.--Comparison of "sawdust snow" catch in model Standard Gage operating under various windshield combinations.

type of windshield	actual amount of sawdust caught in storm period (gms)
none	5.8
none	5.2
Nipher	7.6
Nipher	7.9
Original Alter	10.4
Original Alter	11.0

As pointed out by Weiss and Wilson (1958) the range of expected validity of shields must be considered. Normally a gage is subjected to a wide range of turbulent airflow patterns. Eddies on the order of hundreds of feet are created by ridges, large buildings and tree lines. Smaller trees, buildings and brush produce eddies on the order of a few feet. Gage sites that are characterized by small turbulent patterns (on a scale of inches) must be rather open with little surrounding obstructions. Only when small turbulence patterns exist can a gage shield be expected to perform well. A shield is principally useful for reducing or eliminating the eddies produced by the gage itself and in reducing the vertical components of the air passing over and around the gage.

When evaluating the catch effectiveness of a shielded gage it must also be kept in mind that the standard of comparison itself is subject to uncertainties. The USWB Standard Raingage without shield is usually used as a comparison for rainfall measurements. In snow measurement comparison is often made with the snow depth in the area surrounding the gage site.

Drop Characteristics

Blanchard (1948) concluded that water drops less than 4.6 mm in diameter are quite stable, that those between 4.6 and 5.4 mm are increasingly unstable, and that those over 5.4 mm in diameter will break up if subjected to a shock. Leonard (1904) concluded that drops over 5.5 mm in diameter cannot exist for more than a few seconds. However, Umback and Lembke (1966), experimenting with drops falling through a 12 foot high section of a wind tunnel, found that 5.5 mm drops did not break up when subjected to a 20 fps crosswind. They concluded that "the shock imposed on a drop of this size by this magnitude of wind, and the short fall distance involved, was apparently insufficient to cause breakup."

Green (1952) evaluated the data on terminal velocities published by Laws (1941) and derived the following relation:

$$K = 0.00122\ d^{2.44}$$

where K = force of air resistance in grams,

and d = drop diameter in millimeters.

This relation agreed with Laws' data for drop diameters of 1.17 to 3.92 mm.

Gunn and Kinzer (1949) made an extensive study of the terminal fall velocity of drops of 0.07 to 5.7 mm in diameter. Velocities of drops .08 mm and smaller were found to agree with Stoke's law. Drops over 5.76 mm in diameter were found to be unstable.

Their results have been used to determine the drag characteristics of drops for this study. Further discussion of this matter will be found in the section on experimental design. Their comments on the effect of density or frequency of falling drops indicated that the change in drag characteristics involved were on the order of a few percent.

TABLE 5.--Terminal fall velocity of water drops in air. From Gunn and Kinzer (1949).

drop diameter (cm)	velocity (cm/sec)
0.10	403
0.20	649
0.30	806
0.40	883
0.50	909

EXPERIMENT DESIGN

General Description

The objective of this study was to determine the disturbed airflow pattern in the vicinity of a standard raingage. And to evaluate its influence on the quantity of rainfall measured by the gage.

Velocity measurements were made with an anemometer-analog computer system with raingage models in a wind tunnel. Three dimensional flow field velocity components were measured above and upstream of the raingage models. Thus having a flow field description, and knowing the drag characteristics of water drops, the trajectory of drops approaching the gage could be computed, and the proportion of drops that were intercepted or those that were deflected from the gage's opening could be determined. The factors influencing the falling drop's path included: the constant force of gravity, the drag forces due to the drop's movement through the air, and the mass momentum of the drop.

As the variety of turbulence patterns found at normal raingage sites are numerous, and as they have not been described, the gage was placed in a uniform flow field of a wind tunnel to determine the local air disturbances created by the raingage itself.

The result expected from this experiment was a relation between the proportion of drops intercepted by the gage, the size of the falling drops and the local airflow velocity.

Theoretical Approach

A theoretical approach to evaluating and describing the flow field around a raingage could be obtained by applying the Navier-Stokes equations. In the cylindrical coordinate system the three dimensional Navier-Stokes equation set is

$$\frac{\partial u}{\partial t} + u\frac{\partial u}{\partial r} + \frac{v}{r}\frac{\partial u}{\partial \phi} + w\frac{\partial u}{\partial z} - \frac{v^2}{r} = -\frac{1}{\rho}\frac{\partial P}{\partial r} + \nu\left[\nabla^2 u - \frac{u}{r} - \frac{2}{r^2}\frac{\partial v}{\partial \phi}\right]$$

$$\frac{\partial v}{\partial t} + u\frac{\partial v}{\partial r} + \frac{v}{r}\frac{\partial v}{\partial \phi} + w\frac{\partial v}{\partial z} + \frac{uv}{r} = -\frac{1}{\rho r}\frac{\partial P}{\partial \phi} + \nu\left[\nabla^2 v + \frac{2}{r^2}\frac{\partial u}{\partial \phi} - \frac{v}{r^2}\right],$$

$$\frac{\partial w}{\partial t} + u\frac{\partial w}{\partial r} + \frac{v}{r}\frac{\partial w}{\partial \phi} + w\frac{\partial w}{\partial z} = -\frac{1}{\rho}\frac{\partial P}{\partial z} + \nu\,\nabla^2 w\,,$$

where $\nabla^2 = \frac{\partial^2}{\partial r^2} + \frac{1}{r}\frac{\partial}{\partial r} + \frac{1}{r^2}\frac{\partial^2}{\partial \phi^2} + \frac{\partial^2}{\partial z^2}$,

u,v,w = the velocity components along the x, y, and z axis, respectively,

r,ϕ,z = cylindrical coordinates,

ρ = fluid density,

t = time,

P = pressure,

and ν = fluid viscosity.

These equations can be simplified somewhat by assuming uniform flow conditions, that is

$$\frac{\partial u}{\partial t} = \frac{\partial v}{\partial t} = \frac{\partial w}{\partial t} = 0.$$

This condition cannot be expected downstream and immediately above the cylinder, where turbulent flow will exist for all but the lowest free stream velocities. If R, the cylinder's radius, can be considered small then it may also be possible to let $\partial P = 0$.

Figure 1 illustrates the coordinate system used for this equation set, and a simple cylindrical "raingage."

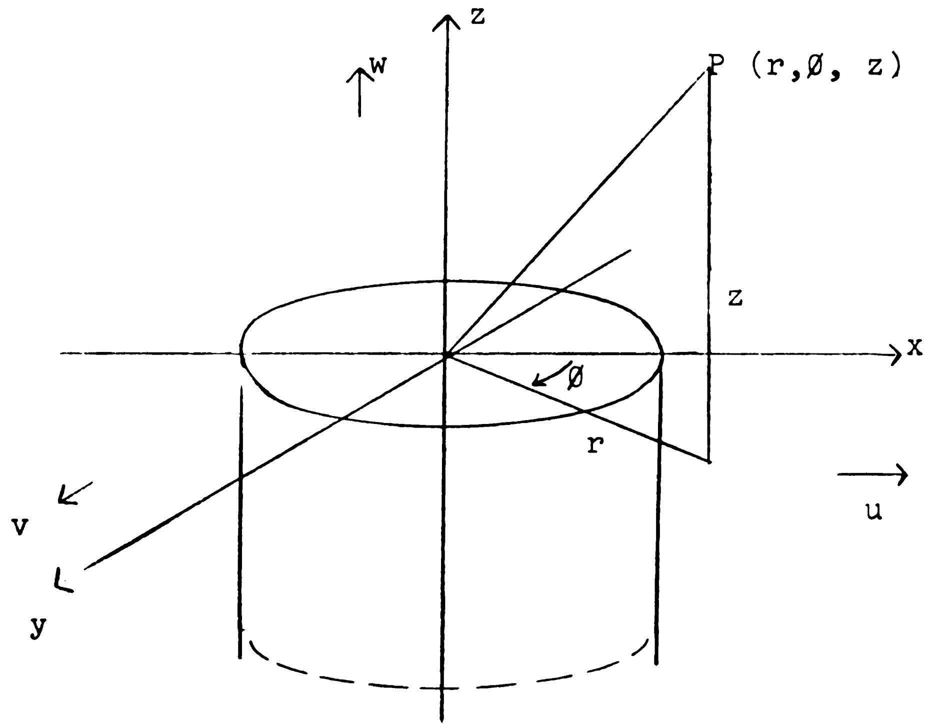

Figure 1.--Cylindrical coordinate system and simple cylindrical "raingage."

The boundary conditions for the Navier-Stokes equations are:

$$u = v = w = 0 \text{ when } z < 0 \text{ and } r = R,$$

and $v \to 0$, $w \to 0$ and $u \to V_\infty$ as $r \to \infty$,

where V_∞ is the uniform horizontal flow field velocity.

An attempt was not made to solve these equations, because when they were simplified to the point where a solution could be found with today's mathematical tools, they no longer described the problem adequately.

The possibility of finding a solution by simulation on an analog computer has been considered. As differentials must be with respect to time for solution on analog computers, the Navier-Stokes equation set must be converted so all partial derivatives are with respect to ∂t or ∂t^2. After multiplying by $\frac{\partial^2 r}{\partial t^2}\frac{\partial^2 \phi}{\partial t^2}\frac{\partial^2 z}{\partial t^2}$, collecting like terms and simplifying, the equation set is

$$z''\left\{\phi''\left[u'r'(u-\frac{\nu}{r})-r''(\frac{v^2}{r}-\frac{\nu u}{r})-u''(\nu+\frac{\nu}{r^2})\right]+r''\phi'\left[\frac{v}{r}u'-\frac{2}{r}v'\right]\right\}$$

$$= r''\phi''(\nu u''-wu'z'),$$

$$z''\left\{\phi''\left[v'r'(u-\frac{\nu}{r})-r'\frac{v}{r}(u\frac{\nu}{r})-v'(\nu+\frac{\nu}{r^2})\right]+r''\phi'\left[v'\frac{v}{r}-u'\frac{2}{r^2}\right]\right\}$$

$$= r''\phi''(\nu v''-wv'z'),$$

$$z''\left\{\phi''\left[w'r'(u-\frac{\nu}{r})-w''(\nu+\frac{\nu}{r^2})\right]+\frac{v}{r}w'r''\Phi'\right\} = r''\phi''(\nu w''-ww'z').$$

These equations would require an analog computer having

12 integraters, 49 multipliers and at least 60 operational amplifers, plus auxiliary equipment.

Cylinder Drag Characteristics

As the coefficient of drag of a truncated cylinder is constant for:

$$1.5\ (10)^4 \leq \text{Reynolds number} \leq 2\ (10)^5$$

the flow field description would remain constant for a cylinder (or a simple cylindrical raingage) subjected to a flow field of a velocity producing a Reynolds number within this range. For an eight inch standard raingage this is equivalent to a velocity range of approximately:

$$3 \leq \text{Velocity (fps)} \leq 50.$$

Thus a relation of catch, drop size and flow field velocity could be obtained over this range by studying the flow field configuration at one velocity within this range.

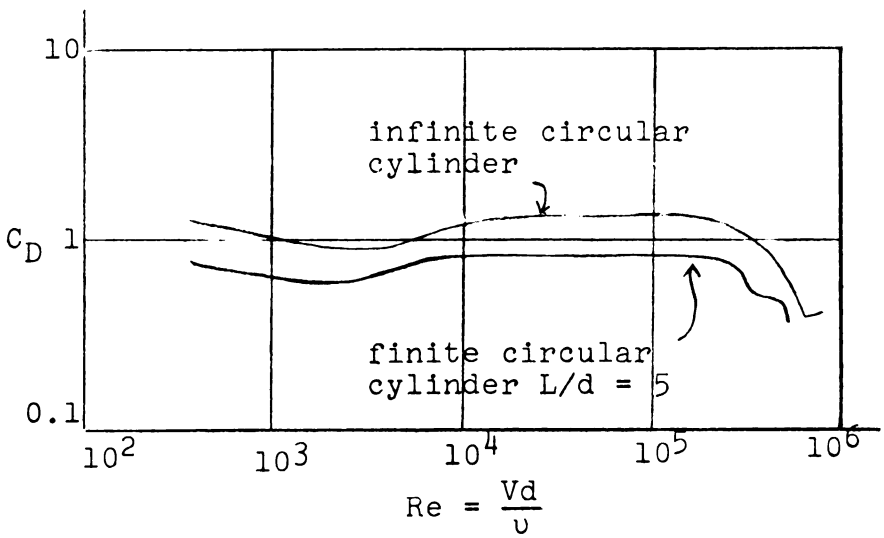

Figure 2. Aerodynamic drag characteristic of a truncated cylinder as a function of the Reynolds number.

Falling Drop Characteristics

Several researchers have investigated the drop size distribution found in various types of rainfall. Most have found that drops of 1 to 1.5 mm in diameter occur most frequently in all but the more intense thunderstorms. Drops of 3.5 to 4.5 mm have been the largest commonly found. In this report drops of 1, 2, 3 and 5 mm in diameter have been considered.

The drag coefficient of a drop can be determined by applying the equation:

$$F = \frac{1}{8} \pi \rho_a d^2 V_r^2 C_d$$

where F = drag force,

ρ_a = air density,

d = drop diameter,

V_r = relative drop velocity,

C_d = coefficient of drag.

The drops' weight can be computed from:

$$W = \frac{1}{6} \pi d^3 g (\rho_w - \rho_a)$$

where ρ_w = water density.

When a drop is falling at its terminal velocity its weight equals the drag force acting on it. Thus, the two above equations can be equated to obtain:

$$C_d = \frac{4}{3} g \frac{\rho_w - \rho_a}{\rho_a} \frac{d}{V_r^2}$$

The coefficient of drag was determined by applying the terminal velocity of drops as found by Gunn and Kinzer (1949).

Air density at 20° C, 1 atmosphere pressure and 50 percent relative humidity, and water density at 20° C were used for these calculations.

Tunnel Wall Corrections

In order to compensate for the constricting effect of the wind tunnel walls, certain corrections must be made on the velocities measured in the tunnel. These corrections are generally termed wall corrections.

The principle correction needed for the flow field description is to compensate for the lateral constraint of the flow pattern around the model. This is usually called "solid blocking." The presence of the model in the test section reduces the cross-sectional area through which the air must flow and, by Bernoulli's principle, results in increased velocities around the model which must be compensated for.

A second necessary correction is for "wake blocking." Any body without boundary layer control creates a wake. This wake has a mean velocity lower than the free stream velocity. To conform to the law of continuity the velocity outside of the wake in a closed tunnel must be greater than the average free stream velocity. This increased velocity in the portion of the stream outside of the wake results in a lowered pressure which in turn produces a pressure gradient and an airflow velocity increase around the model.

Streamline curvature is a third error that is created by the constraining influence of the tunnel walls. While this effect is a result of solid blocking, it is usually treated separately in the study of airfoils.

Another correction that is commonly made in wind tunnel tests is that for "buoyancy." Most tunnels have a variation of static pressure along the test section due to the thickening of the walls' boundary layers, which results in increased velocities as one traverses the test section's length. This pressure gradient tends to "draw" the model downstream. The tunnel used in this study has a tapered test section to compensate for the boundary layer buildup, thereby minimizing the need for buoyancy corrections.

These wall corrections can be experimentally verified by testing several models of different sizes of the same subject at the same Reynolds number. This procedure also provides a second method of evaluating wall corrections which encompasses all of the above error terms in one correction. By determining the ratio of the measured velocity at a point to the free stream velocity for each of the two or more models, a dimensionless curve of velocity ratio versus model scale can be made. By extrapolating the curve that passes through these points to the ordinate position, where the model scale equals zero, one finds the velocity ratio that would exist with a prototype subject in a nonconstrained flow field. This is illustrated in Figure 3. That is, the surrounding flow field size to model size ratio approaches infinity, which is the condition found in the normal prototype subject use.

Data from two models of different scales can be used similarly, for which a straight line is used in the extrapolation process. Three models create three points on the graph and allow the use of a second order curve which improves the accuracy of this method. This method of correcting the flow field data has been used to correct the data presented in this report.

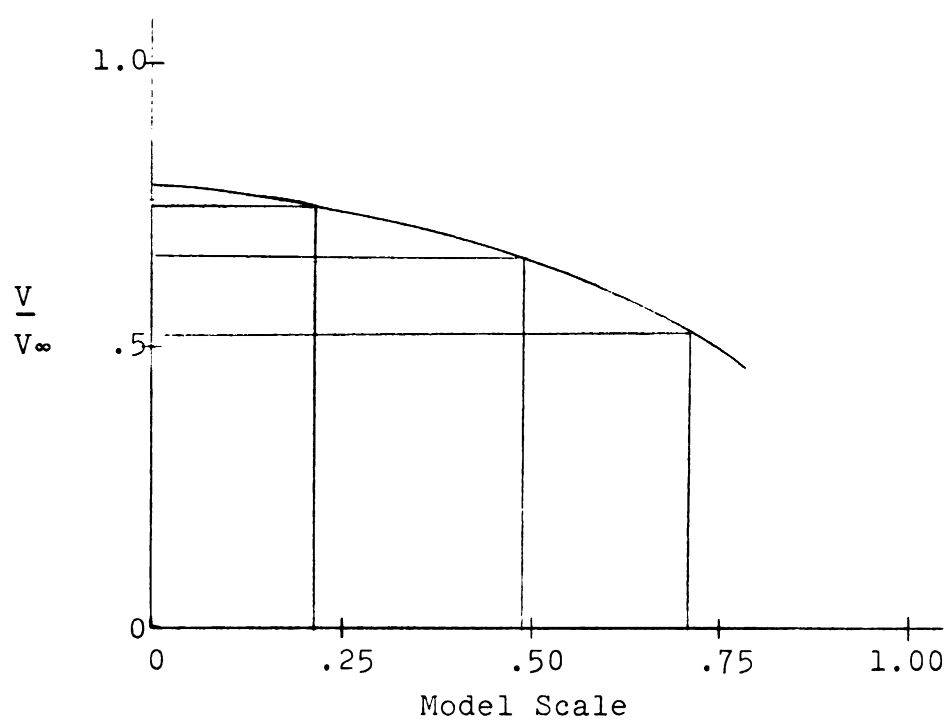

Figure 3.--Wind tunnel correction curve using three data points.

Data Collection Points

A three dimensional grid of data collection points was oriented above and upstream from the model. Spacing of all grid points was d/4, where d is the model's top inside diameter. The grid extended to the top of the test section's uniform flow area, horizontally to d/4 beyond the gage edge, and upstream for 25 intervals, or until a nearly uniform flow field was encountered. Thus, the coordinate indices limits were:

$1 \leq x \leq 4$ - horizontally, cross-stream direction,

$1 \leq y \leq 15$ - vertical direction,

$1 \leq z \leq 25$ - upstream direction.

The x = 1 plane passes through the cylinder's vertical axis and is parallel to the free stream flow direction. The y = 1 plane is horizontal, d/8 below the cylinder's top edge, and parallel to the free stream flow direction. The z = 3 plane is normal to the flow field, is vertical, and passes through the vertical axis of the cylinder.

Three models of different sizes were used in the wind tunnel tests, which resulted in three different spacings of the data collection points. Thus the number of data points along the vertical (y) axis varied with each model. Due to this, the number of points used to find the velocity ratio for various grid points varied. All grid points up to $y = 8$ above the gage had 3 values for extrapolation purposes.

When measuring the flow field several diameters upstream of the model, where the flow field was nearly uniform, intervals of $d/2$ were used in the z direction.

When the data set collected in the wind tunnel was subsequently used for computations the model's coordinate system was moved 3 intervals in the negative x direction. This allowed sequential numbering of the yz planes when the data values were reflected about the model's center yz plane to obtain a data field for the full width of the gage.

Data Interpolation

The data values used for drop trajectory computations were in the form of velocity ratios. These ratios being the velocity component parallel to a model axis at a data point divided by the free stream velocity. Thus, any free stream velocity could be considered by using velocity ratios derived from the basic data.

To determine the velocity component ratios at positions other than at data collection points it was necessary to interpolate between the known values. This was done in the three dimensional data array by repetitive application of a one dimensional interpolation procedure.

Interpolation was accomplished by using the Newton interpolation formula based on divided differences, Hamming (1962), using data from four grid points, two on each side of the point in question. This procedure, in effect, finds a third order polynomial and evaluates it at that point.

To find the unknown velocity ratio at a desired point x (refer to Figure 4) in a three dimensional array of data this procedure was first applied in the y direction for two points above and two points below the XZ-plane that point x lies in. This determines the velocity ratios at 16 positions surrounding the point x, on the XZ-plane (points "a" in Figure 4).

Interpolation was then carried out in the x direction. Four of the points found in the previous step were used to find the velocity ratios on a line parallel to the z-axis that passes through point x. This was done four times to find four values along this line, two toward the origin and two away from the origin, from point x (points "b" in Figure 3). By interpolating once more along this line, which is parallel to the Z-axis, the velocity ratio at point x was found.

When drops approached the edge of the data field it was not possible to use a third order equation based on four data points. When this condition was encountered, that is, when drops approached the bottom or the down stream end of the data field, a procedure similar to that stated above was used, using three data points and second order interpolation.

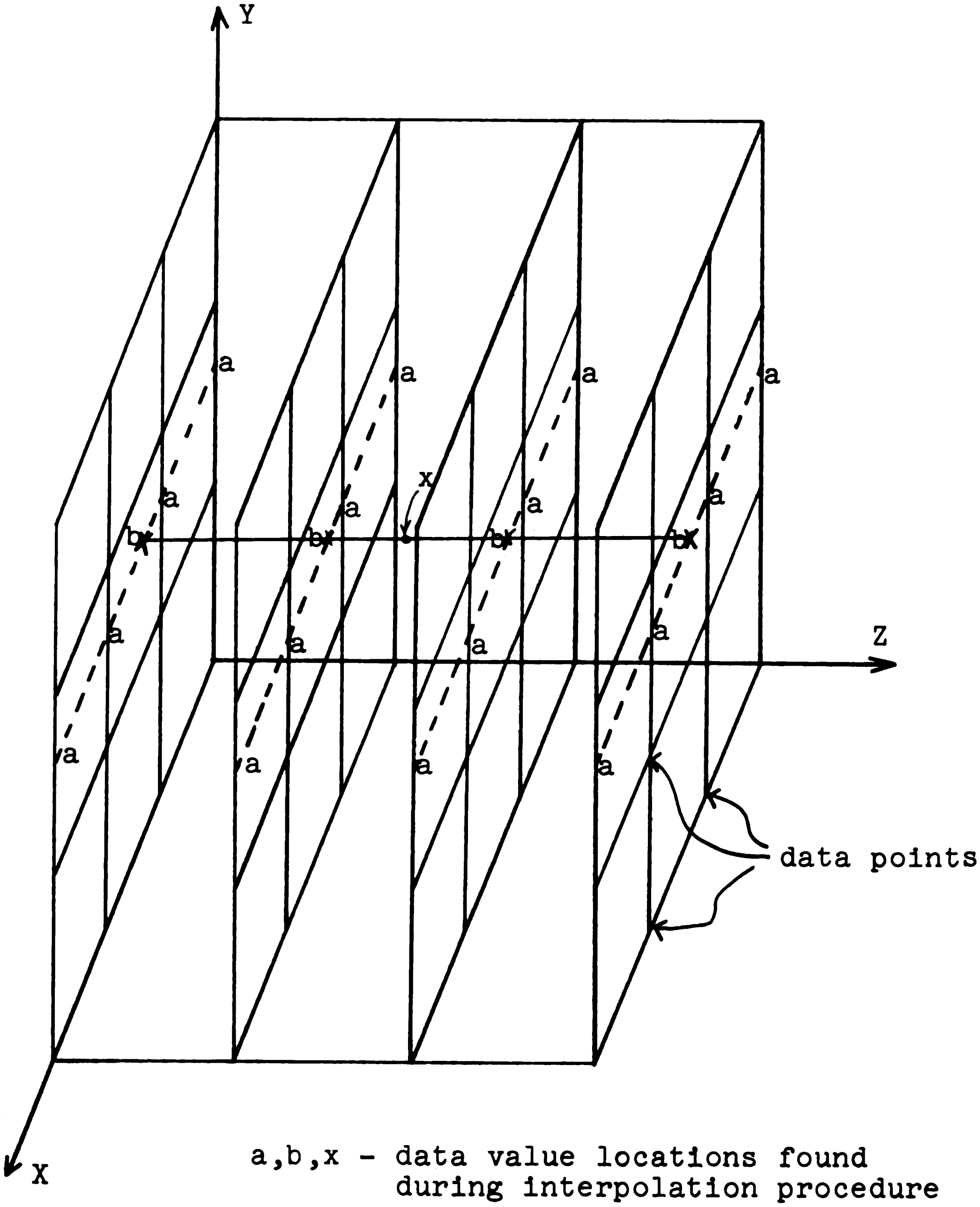

Figure 4.--Interpolation pattern to determine unknown velocity ratio at point x.

Drop Catch Area

The area defined as the drop catch area is that portion of the high shear or boundary layer immediately above the gage's funnel opening. A second velocity data set was collected, using intervals of $\Delta y = d/16$ and $\Delta x = \Delta z = d/8$, in the immediate vicinity of the gage funnel. By observing the change in velocity between adjacent data collection points it was possible to define the boundary layer's position above the gage's funnel opening. Using this information the boundary layer was simulated by using segments of 17 plane surfaces. The surfaces used, and their limits are defined in function CATCH of program DROPPATH (refer to Appendix B).

Velocity measurements below the boundary layer showed that low mean velocity and highly turbulent flow was predominate. Since the drop masses were relatively large as compared to the forces applied to the drops by the turbulent air below the boundary layer, and since the drop reaction decreases as the frequency of the applied force increases, it was assumed that the drops that passed through the boundary layer were not deflected by the air movements in that region. Thus, once drops had passed through the boundary layer their paths depended primarily on their velocity and movement direction as they passed through the boundary layer.

Since the boundary layer was a positive distance above the gage's opening (except along the upwind edge) it was possible for a drop to pass through the boundary layer above the cylinder and still miss the gage's funnel if the drop's trajectory was such that it could pass over the edge of the funnel. The possibility of this occurring was allowed for in program DROPPATH.

Data Conversion

Several FORTRAN computer programs were developed to handle and analyze the data collected in the wind tunnel tests.

Program TURB

Program TURB is a tape handling routine which transfers the three coordinate positions and the three velocities indicated by the anemometer, from paper tape to magnetic tape in binary form for ease in further processing.

Program MAIN

Program MAIN was used to convert the binary data on the magnetic tape to the base ten number system and to provide a print out of the basic data. MAIN also punched the six values of each data point along with an identifying number onto computer cards for future use.

Program TRANS

This program served two purposes. From microphotographs of the sensor probe, the average angle between each sensor and the plane of the other two sensors was measured. Program TRANS calculated the resulting angles between the sensors and the model coordinate system. Using this information, TRANS then computed the three velocity components parallel to the model axis system at each data collection point from the data obtained from program MAIN.

Indicated flow velocity across an anemometer sensor is not directly proportional to the sine of the angle between the flow direction and the sensor's axis. Therefore an additional correction was made to compensate for this crossflow effect by the equation:

$$V_p^2 = V_i^2 (\sin^2\alpha + K^2 \cos^2\alpha)$$

where V_p = true velocity component perpendicular to sensor axis,

V_i = indicated velocity,

α = angle between flow direction and sensor axis,

K = correction factor.

The value of K was determined for each sensor in the primary instrument calibration procedure.

Program CORRECT1

Errors in the basic data that were caused by slight misalignment of the anemometer probe were compensated for in this program. Probe misalignment was determined by making velocity measurements at selected points in the wind tunnel after the model had been removed. The velocity components measured in the cross stream and vertical directions were then subtracted from the data taken with the gage in the tunnel.

Program CORRECT2

To compensate for the influence of the tunnel walls on the flow field, corresponding flow components collected at each data point for each model tested were used to find the corrected velocity component at that point. The method used is described in the section Tunnel Wall Corrections.

Program DROPPATH

From Gunn and Kinzer's (1949) data, the influence of relative airflow on movement was mathematically described. Combining this force as a function of the local flow field velocity and direction with the influences of gravity and inertial forces, a stepwise progression of a falling drop's trajectory was determined. DROPPATH simulated rainfall using several drop sizes commonly found in rainfall and several airflow velocities in the 3 to 50 fps range.

Flow field characteristics between data points were usually determined by third order, three dimensional interpolation. Near the edge of the data field second order interpolation was used.

Drop fall starting points were distributed in the y = 14.5 plane at intervals of d/16 in the x and z directions. The drop was given an initial velocity of the terminal velocity for its size plus the air velocity components at its starting point. This simulated the drop's travel path as if it had been falling through a uniform flow field similar to that found at its starting point. By comparing the number of drops intercepted by the gage with the number starting in an area of the same size on the y = 14.5 plane the percentage of catch was determined for several common drop sizes.

APPARATUS

Wind Tunnel

The wind tunnel used for model testing is owned and operated by the Mechanical Engineering Department at Michigan State University. This tunnel is of the constrained suction type with a 25:1 constriction ratio and a test section 2 ft by 2 ft by 10 ft long. The variation of velocity across the test section is less than 2 percent outside of the boundary layer. The test section has a lengthwise taper to compensate for the boundary layer buildup and to minimize the need for bouyancy corrections. The variable pitch fan and motor control system provide excellent control and stability of flow velocities.

A Prandtl tube mounted to one side and slightly upstream of the model was used to constantly monitor the tunnel air velocity during tests with the aid of a sloping tube water manometer. A mercury column barometer and thermometer in the laboratory provided data to correct the manometer readings for atmospheric changes.

Anemometer

A three channel constant temperature hot film anemometer system was used for three dimensional flow field measurements. The sensing probe held the three hot film sensors in a pyramid formation. The angles between the sensors were approximately 100 degrees. Three temperature compensating probes were placed in the downstream end of the tunnel's test section to provide automatic anemometer compensation for air temperature changes.

Two rack and pinion gear driven hook gages with scales were modified to manipulate the probe in the horizontal (cross stream) and vertical directions. The base holding these gages was moved along the tunnel test section to obtain a longitudinal placement. Probe placement accuracy was ± .006 inch (.0005 ft).

Analog Computer

The three bridge voltages from the anemometer modules were fed to an analog computer. This computer provided signal conditioning, conversion of anemometer bridge voltage to the related velocity (linearization), and real time integration to obtain mean velocities normal to each sensor element.

From each bridge voltage, a voltage equal to the bridge output at zero velocity was subtracted. The resulting signal was multiplied by a constant to obtain a 10 volt signal when an anemometer sensor was normal to a 100 fps flow field. This conditioned signal was fed to a variable diode function generator (VDFG) which converted the 0 to 10 volt range such that:

$$E'_o = 0.100 \times \text{Velocity (fps)}.$$

The VDFG was adjusted with the anemometer calibration data obtained from the instrument's primary calibration to allow for variations in individual bridge and sensor characteristics.

This voltage (E'_o - a function of velocity) was divided by 10 and then summed by an analog integrator over a 10 second period to obtain a mean velocity value. Three of these circuits were used to convert the three anemometer bridge voltages.

An independent square wave generator operating at 0.0500 Hz was used to control the time period of integrator operation.

Data Recording

Three variable voltage sources were used to provide probe position data. These were adjusted to correspond to the anemometer probe's position. These three voltages, along with the three analog output voltages were fed to an analog-digital converter and paper tape punch. Thus, the probe's coordinate positions, X, Y and Z, and the anemometer's indicated velocities, V_1, V_2 and V_3, were recorded on the paper tape when the converter's remote start scan switch was actuated.

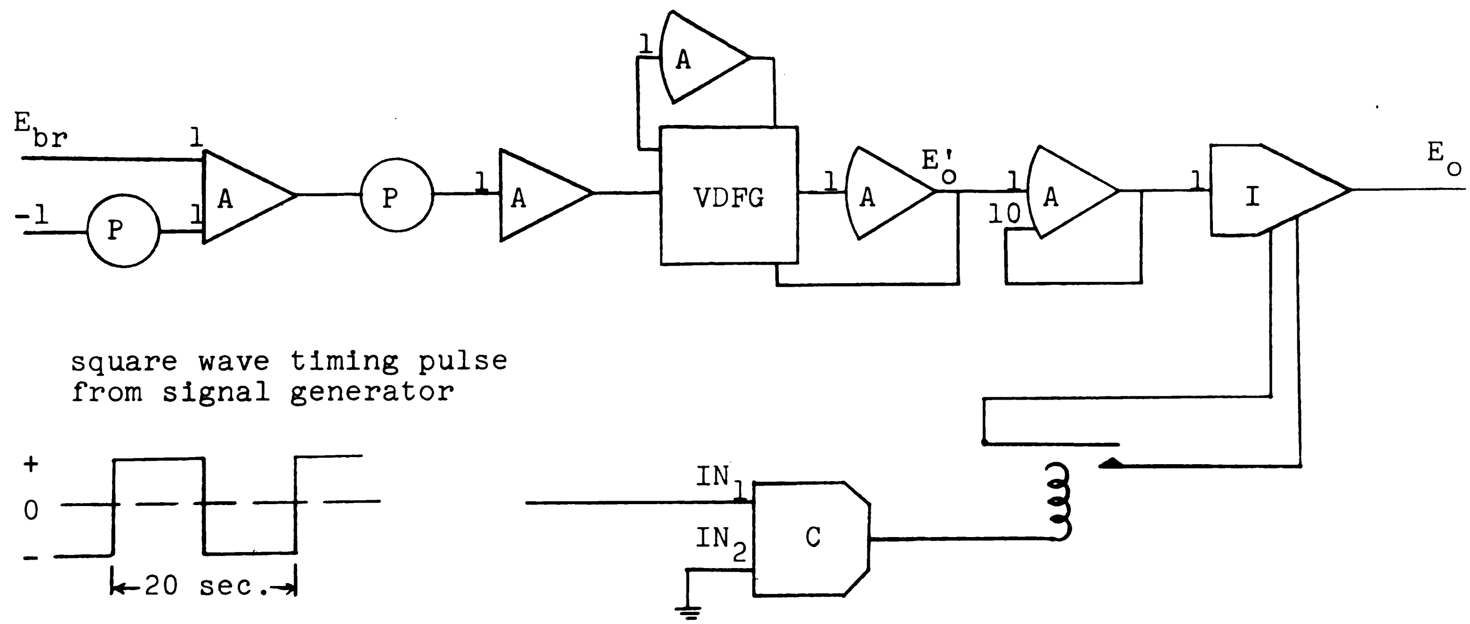

A - operational amplifier

C - comparater

I - integrator

P - potentiometer

VDFG - variable diode function generater

E_{br} - anemometer bridge voltage

E_o - linearized anemometer signal

E'_o - VDFG output voltage

Figure 5.--Analog computer circuit for anemometer bridge output conditioning and linearization.

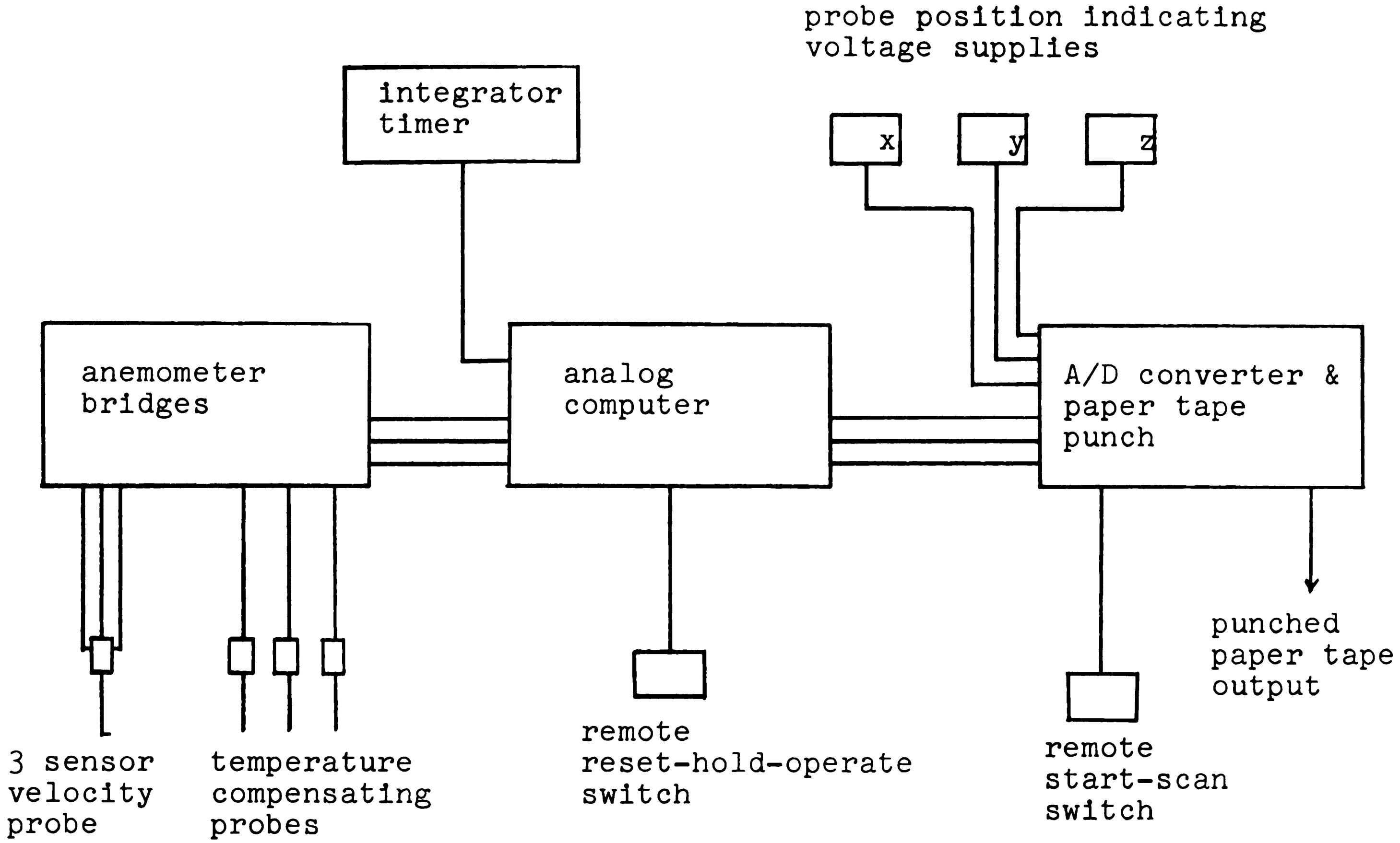

Figure 6.--Flow field velocity measurement instrumentation system.

Raingage Models

Three models of the USWB Standard Raingage with the steel tripod stand were constructed for tests to be conducted in the wind tunnel. Their linear scales, relative to a prototype standard gage, were .704, .490 and .227. As the full height of the largest model could not be facilitated in the wind tunnel due to the tunnel's size limitation, its lower end was truncated such that the top centers of the models were positioned at the vertical and horizontal center point of the tunnel test section.

As the smallest model's height was less than the tunnel floor to center point distance, a ground plane was constructed to maintain a normal gage to ground surface relation and bring the model's top to the tunnel's center point. This allowed the use of a complete model gage with stand. The ground plane, in effect, raised the floor of the tunnel to its height.

The model cylinders were machined from cast acrylic plastic, to a tolerance of ± 0.001 inch. The gage stands were fabricated from cold rolled steel of the proper scale size to a tolerance of ± 0.002 inch.

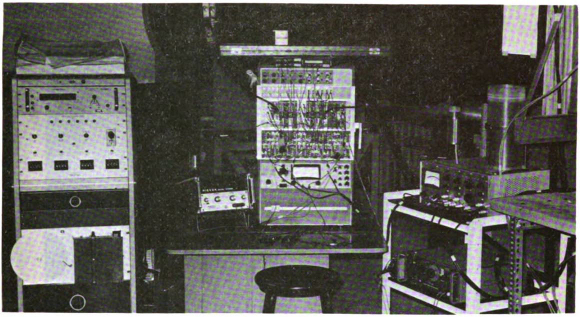

Figure 7.--Velocity measurement instrumentation. Left to right: the analog-digital converter with paper tape punch, digital voltmeter, analog computer, anemometer with the analog timer below it.

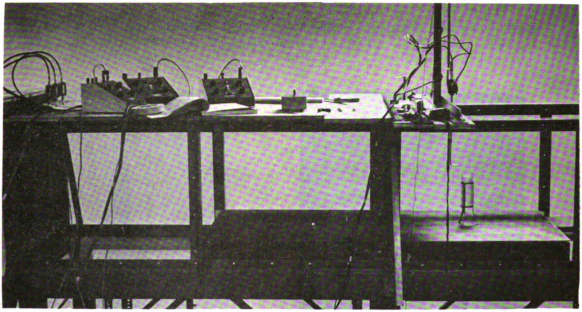

Figure 8.--Wind tunnel test section. Along the top of the test section, from left to right: the three temperature compensating probes, the three probe position indicating voltage sources, the remote switches controlling the computer and A/D converter, the probe manipulator with sensor probe. Within the test section the smallest model is shown mounted on its ground plane.

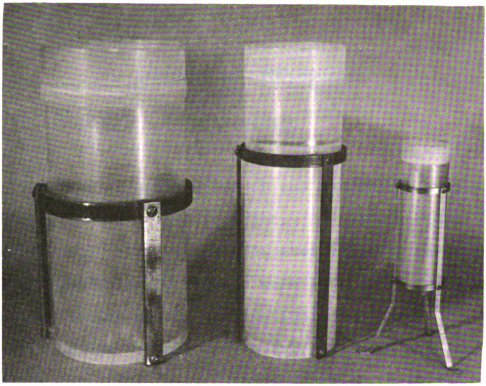

Figure 9.--Gage models used for wind tunnel tests. Model scales, from left to right, are: .704, .490 and .227.

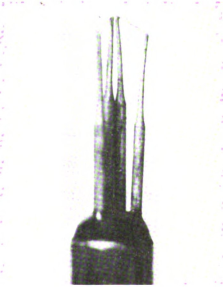

Figure 10.--Anemometer sensor probe, side view.

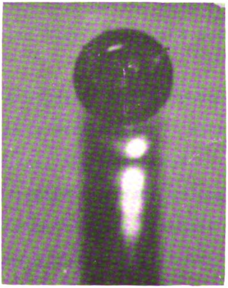

Figure 11.--Anemometer sensor probe, front view.

EXPERIMENTAL PROCEDURE

Calibration

The initial calibration of the anemometer system was made with a one inch free jet. Curves of bridge voltage versus velocity and indicated velocity versus angle of flow over the sensors were determined for each anemometer bridge-sensor combination.

The bridge voltage versus velocity data was used to adjust the VDFGs in the analog computer to obtain automatic linearized bridge voltage to velocity conversion. The velocity versus angle of flow curve was used to evaluate the correction factor (K) used in computer program TRANS which compensated for angled flow across the anemometer sensors.

The three sensor probe was mounted in the probe manipulator and placed in the empty wind tunnel. With a moderate flow velocity in the tunnel the probe was oriented so that all sensors indicated the same velocity to insure that the sensors were symetrically oriented to the uniform flow field. Next the signal conditioning portion of the analog computer circuit was adjusted so that the VDFG's output voltage was zero at zero flow velocity, and was 10.000 times the sine of the sensor-flow direction angle at 100 fps. The external square wave signal generator for the timing circuit was adjusted so that the integrator output voltage equaled ten times its input voltage.

Following the initial instrumentation calibration the desired model was mounted in the tunnel and the probe was adjusted to a known reference point, that is, a data collection grid point relative to the model.

The tunnel operating velocity was monitored with a Prandtl tube and a sloping tube water manometer. The desired dynamic-static pressure head differences was computed periodically and velocity adjustments were made if needed. The desired pressure head difference was computed from the ambient air temperature, barometric pressure and the desired Reynolds number. All tests were run at $Re = 7\ (10)^4$.

After velocity measurements were made at all data collection points the model was removed from the tunnel and velocity measurements were repeated on the z = 1, 12 and 25 planes as a check for proper probe orientation and flow uniformity. Any deviations found were corrected for in computer program CORRECT1 with this information.

Test Routine

After mounting the desired model in the wind tunnel, the probe was positioned at a reference point and the desired operating velocity was established.

The normal sequence for data collection was:

1. position probe at desired x, y and z coordinate,
2. place analog computer in operate mode allowing timer to operate integrators for 10 second period,
3. adjust variable voltage sources for proper x, y and z values to be recorded,
4. At end of timer cycle initiate scan cycle of A/D converter and paper tape punch to record the three coordinate values and the three velocities measured with the anemometer,
5. reset the analog integrators to zero,
6. repeat the above steps at the next data collection point.

DISCUSSION OF RESULTS

To make use of this study's results the accuracy of the procedures used must be considered.

A precise analysis of the errors involved in this study was precluded by the presence of several unknown possible errors in many of the procedures used. However, the major source of error is probably in the basic velocity measurements made.

An estimate of the errors involved in the velocity measurements can be obtained by considering past experiences by researchers using basically the same instruments and techniques under similar conditions. In the area of fluid mechanics, mean velocity measurements using hot wire anemometers are generally considered to be within 10 percent of the actual flow velocities. The use of check procedures, such as the probe alignment correction made by program CORRECT1, will reduce this error. However, by combining several instruments to handle the data, such as the analog computer and analog-digital converter used in this study, the maximum error probably remains in the vicinity of 10 percent.

The largest error source in the computations using the velocity data would be in the iteration portion of program DROPPATH that determines the path that a drop follows due to the influence of its surrounding velocity field. This error source was minimized by running test programs using several drop sizes and free stream velocities and by varying the time interval (DT in program DROPPATH) of the iteration process. It was found that a DT smaller than 0.002 second made negligible difference in the drops' path descriptions. Thus, a time interval of 0.002 second was used.

Considering these factors and the confidence in the procedures used it is estimated that the results of this study (Figure 12) are not in error by more than 15 to 18 percent.

A comparison of the drop paths showed a tendency for drops that were caught by the gage to be carried further from the upstream edge of the gage as the free stream velocity increased and as the drop size decreased. This trend was expected. However, this trend of being displaced downstream was also evident with drops falling to the level of the gage's top but slightly in front of and to one side of the gage funnel. This tendency can increase the gage's catch. This is the direct result of the gage's obstruction to airflow in its vicinity due to the physical presence of the gage itself. While the quantity of drops

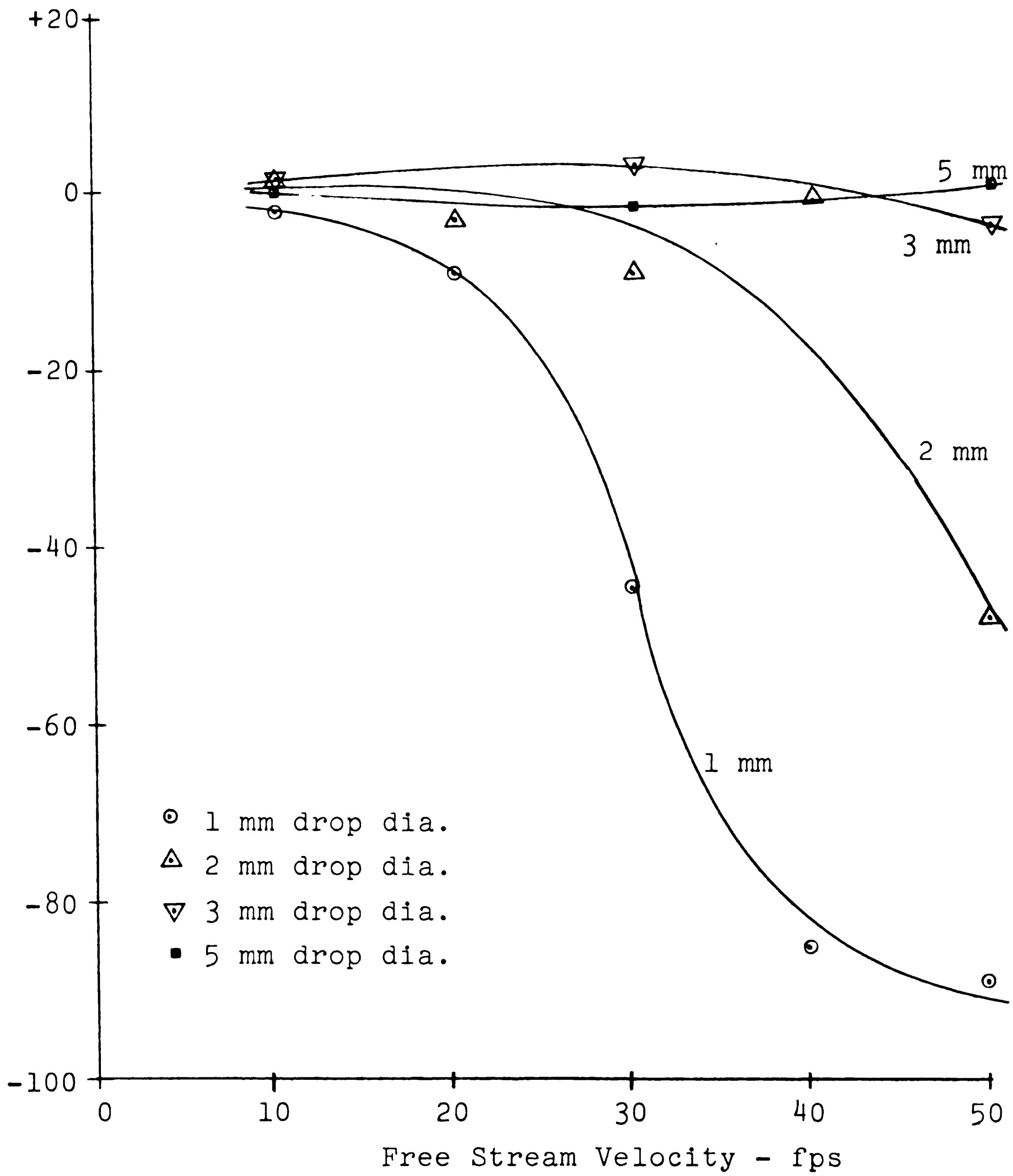

Figure 12.--Percent error of drops caught relative to drop diameter and free stream velocity.

influenced by this trend is small, it is probably responsible for the small increase in catch of the larger drops at free stream velocities in the neighborhood of 20 to 40 fps.

As drop size decreases to 1 mm, this trend resulted in most drops being caught in the downstream side of the gage. As free stream velocities increase beyond 20 fps most of these smaller drops were carried beyond the gage funnel before they fell to the level of the gage's top, resulting in a sharp decrease in the quantity of drops caught. This effect is very pronounced for 1 mm diameter drops in the 30 to 50 fps range as shown in Figure 12.

As drops in the 1 to 2 mm size range occur most frequently in normal precipitation, and as they account for a large portion of the total volume of rain falling, the error created can be large if the free stream velocities are above 25 fps.

To use this data one needs to know the drop size distribution of the rainfall, and to measure the free stream velocity in the gage's vicinity during the rainfall period. The portion of drops of each size falling is then adjusted with the values found in Figure 12 to find the corrected portion of each drop size. Summing the volume of the adjusted amount of each drop size will then determine the corrected precipitation quantity.

CONCLUSIONS

The results of program DROPPATH showed that rainfall measurements made with a U. S. Weather Bureau Standard Raingage indicate less rainfall than actually fell as the drop diameter decreases and as the free stream air velocity in the gage's vicinity increases.

At velocities over 30 fps the amount of 1 mm diameter drops caught was in error by over 40%. At 40 fps the 1 mm diameter drops measured were in error by 80% and 2 mm diameter drops were in error by approximately 20%. As a large portion of the drops in a typical rainfall is usually within this size range, rather large errors should be expected in the amount of rainfall indicated by a Standard Raingage if wind velocities are over 30 feet per second.

While the results of this study could be applied to rainfall data that has been collected it should also be considered as an indicator of the need for development of an improved precipitation measurement system.

REFERENCES

REFERENCES

Alter, J. C. (1937). Shielded storage precipitation gages. Monthly Weather Review 65: 262-265.

Bernard, M. (1938). The expanded program of the U. S. Wea. Bu. in snow-work. Trans. Amer. Geo. U., Regional meeting, January.

Blanchard, D. C. (1948). Observations on the behavior of water drops at terminal velocity in the air. Occasional Rept. No. 7, Project No. 7, Project Cirrus, G. E. Res. Lab., Schenectady, N. Y.

Borstein, R. (1884). Ueber der von Nipher vorgeschlagenen Schutztrichter fuer Regenmesser. (Concerning the protecting funnel suggested by Nipher for rain-gages). Meteorologische Zeitschrift Band I Berlin 1: 381-392.

Conover, J. H., and T. G. Nastos (1951). Tests of Steward and Victor precipitation gages. Blue Hill Report, Harvard University. July.

Gold, E. (1931). The splashing of rain. Meteorological Magazine 63(746): 39-40.

Green, Robert L. (1952). Evaluation of air resistance to freely falling drops of water. Agricultural Engineering 33: 28, 286.

Gunn, Ross and G. D. Kinzer (1949). The terminal velocity of fall for water drops in stagnant air. Meteorology 6: 243-248.

Hamming, R. W. (1962). Numerical Methods for Scientists and Engineers. McGraw-Hill, Inc., New York. 409 pp.

Heberden, W. (1769). Of the different quantities of rain, which appear to fall at different heights, over the same spot of ground. Philosophical Trans. 59: 359-362.

Horton, R. E. (1919). The measurement of rainfall and snow. New England Water Works Assoc. 33(1): 14-72.

Howell, W. E. (1946). Blue Hill Report, Harvard University.

Kurtyka, John C. (1953). Precipitation measurements study. Illinois State Water Survey Div., Report of Investigation No. 20.

Laws, J. Otis (1941). Measurements of the fall velocity of water drops and rain drops. Trans. Amer. Geo. Union 20: 709-721.

Leonard, P. (1904). Ueber Reger. (Concerning Rain.) Meteorologische Zeitschrift 21: 249-262.

Nipher, F. E. (1878). On the determination of the true rainfall by elevated gages. Amer. Assoc. for the Adv. of Science 27: 103-108.

Shamasastry, R., translated by. (1915). Arthasastra. (321-296 B.C.) Government Oriental Library Services, Bibliotheca Sanskrit.

Stevenson, T. (1842). On the defects of raingages with description of an improved form. Edinburgh New Philosophical Journal 33: 12-21.

Symons, G. J. (1871). Notes on foregoing papers. British Rainfall: 56-57.

Umback, C. R., and W. D. Lembke (1966). Effects of wind on falling drops. Trans. of ASAE 6: 805-808.

Warnick, C. C. (1956). Influence of wind on precipitation measurements at high altitudes. Univ. of Idaho, Engineering Expt. Sta. Bull. No. 10.

Weiss, Leonard L., and W. T. Wilson (1958). Precipitation gage shields. Int'l. Union of Geodesy and Geophysics 1: 462-484.

Weiss, Leonard L. (1961). Relative catches of snow in shielded and unshielded gages at different wind speeds. Monthly Weather Review, October: 397-400.

Wild, H. (1873). <u>Yearbook of the Physical Central Observatory in St. Petersburg</u>.

Wild, H. (1885). Einfluss der qualitaet und aufstellung auf die angeben der Regenmesser. (Influence of the quality and exposure on the data from rain gages.) Repertorium fuer Meteorologie, St. Petersburg Commissionare der Kaislerlichen Akademie der Wissen Schaften 9 (9): 1-23.

APPENDIX A

TABLE A1.--Field velocity data. Velocity ratios in the x direction on the x = 4 plane. Values in parentheses are within the gages top boundry layer.

y Coordinate	z Coordinate 1	2	3	4	5	6	7	8	9	10	11	12	13	14	15	16	17	18	19	20	21	22	23	24	25
1							-0.02	-0.05	-0.03	-0.03	-0.01	-0.01	-0.01	-0.02	0.00	0.00	-0.01	0.00	0.00	0.01	0.02	0.02	0.02	0.02	0.02
2	(-0.02)	(-0.13)	(-0.22)	(-0.10)	0.12	0.09	-0.01	-0.04	-0.01	-0.01	0.00	-0.01	-0.01	-0.02	-0.02	-0.02	-0.01	0.00	0.00	0.01	0.01	0.02	0.02	0.01	0.01
3	0.05	0.15	0.03	0.24	0.31	0.16	0.07	0.04	0.02	0.00	0.00	-0.01	-0.02	-0.02	-0.01	0.00	0.01	-0.01	0.00	0.01	0.01	0.02	0.02	0.01	0.01
4	0.12	0.09	0.16	0.22	0.16	0.10	0.08	0.05	0.02	0.01	0.01	0.00	-0.02	-0.02	-0.01	0.00	0.01	0.00	0.01	0.02	0.02	0.02	0.02	0.02	0.01
5	0.05	0.09	0.13	0.18	0.13	0.09	0.08	0.07	0.04	0.03	0.03	0.01	0.00	0.00	0.01	0.00	0.01	0.00	0.01	0.01	0.01	0.01	0.01	0.01	0.01
6	0.08	0.08	0.09	0.09	0.08	0.07	0.04	0.03	0.03	0.02	0.02	0.01	0.01	0.01	0.01	0.00	0.02	0.00	0.02	0.01	0.02	0.02	0.02	0.01	0.00
7	0.07	0.07	0.09	0.11	0.08	0.05	0.08	0.07	0.04	0.03	0.03	0.00	0.01	0.01	0.00	0.00	0.02	0.00	0.02	0.02	0.02	0.01	0.01	0.01	0.01
8	0.08	0.08	0.07	0.07	0.07	0.05	0.08	0.08	0.04	0.04	0.04	0.02	0.02	0.01	0.02	0.01	0.02	0.02	0.02	0.02	0.02	0.02	0.02	0.02	0.02
9	0.03	0.04	0.05	0.04	0.04	0.04	0.05	0.05	0.05	0.05	0.05	0.05	0.05	0.05	0.05	0.05	0.05	0.04	0.04	0.03	0.04	0.03	0.02	0.01	0.00
10	0.02	0.02	0.03	0.02	0.02	0.02	0.02	0.02	0.01	0.01	0.01	0.01	0.01	0.00	0.00	0.00	0.01	0.00	0.00	0.00	0.00	0.00	0.00	0.00	0.00
11	0.02	0.02	0.02	0.02	0.02	0.01	0.01	0.02	0.01	0.00	0.00	0.00	-0.01	-0.01	-0.01	0.00	0.00	0.00	0.00	0.00	0.00	0.00	0.00	0.00	0.00
12	0.01	0.01	0.01	0.01	0.01	0.01	0.00	0.01	0.00	0.00	0.00	0.00	0.00	0.00	0.00	0.00	0.00	0.00	0.00	0.00	0.00	0.00	0.00	0.00	0.00
13	0.00	0.00	0.00	0.00	0.01	0.00	0.00	0.00	0.00	0.00	0.00	0.00	0.00	0.00	0.00	0.00	0.00	0.00	0.00	0.00	0.00	0.00	0.00	0.00	0.00
14	0.01	0.00	0.00	0.01	0.01	0.01	0.00	0.00	0.00	0.00	0.00	0.00	0.00	0.00	0.00	0.00	0.00	0.00	0.00	0.00	0.00	0.00	0.00	0.00	0.00
15	0.00	0.00	0.00	0.00	0.01	0.00	0.01	0.01	0.00	0.00	0.00	0.00	0.00	0.00	0.00	0.00	0.00	0.00	0.00	0.00	0.00	0.00	0.00	0.00	0.00

TABLE A-2.--Field velocity data. Velocity ratios in the x direction on the x = 5 plane. Values in parentheses are within the gages top boundry layer.

	z Coordinate																								
y Coordinate	1	2	3	4	5	6	7	8	9	10	11	12	13	14	15	16	17	18	19	20	21	22	23	24	25
1							0.02	-0.02	-0.03	-0.03	-0.02	-0.02	-0.01	-0.02	-0.01	0.00	0.00	0.01	0.00	0.01	0.01	0.02	0.02	0.01	0.00
2	0.10	(0.07)	(0.32)	(-0.31)	0.25	0.07	-0.02	-0.02	-0.05	-0.02	-0.01	-0.01	-0.01	-0.01	-0.01	-0.01	0.00	0.00	0.01	0.01	0.01	0.02	0.01	0.01	0.01
3	0.12	0.18	0.15	0.19	0.21	0.10	0.03	0.00	-0.03	0.00	0.00	-0.01	-0.01	-0.01	-0.01	0.00	0.01	0.00	0.01	0.01	0.01	0.02	0.02	0.01	0.00
4	0.11	0.13	0.18	0.19	0.15	0.10	0.05	0.03	0.00	0.00	-0.01	-0.01	-0.02	-0.02	-0.01	0.00	0.01	0.00	0.01	0.01	0.00	0.01	0.01	0.01	0.00
5	0.08	0.10	0.16	0.13	0.14	0.11	0.09	0.07	0.03	0.02	0.02	0.01	0.00	0.00	0.00	0.01	0.01	0.01	0.01	0.01	0.01	0.01	0.01	0.01	0.00
6	0.05	0.04	0.09	0.07	0.05	0.07	0.05	0.05	0.03	0.02	0.02	0.01	0.00	0.00	0.00	0.00	0.00	0.00	0.00	0.01	0.01	0.01	0.01	0.00	-0.01
7	0.07	0.08	0.08	0.09	0.08	0.07	0.07	0.05	0.02	0.02	0.03	0.01	0.00	0.00	0.00	0.00	0.02	0.00	0.01	0.01	0.02	0.02	0.01	0.01	0.00
8	0.03	0.05	0.05	0.07	0.05	0.05	0.07	0.05	0.03	0.02	0.03	0.02	0.00	0.01	0.01	0.01	0.03	0.02	0.02	0.02	0.02	0.03	0.02	0.02	0.01
9	0.02	0.02	0.04	0.03	0.04	0.04	0.04	0.03	0.03	0.04	0.03	0.02	0.02	0.02	0.03	0.03	0.03	0.02	0.02	0.02	0.03	0.02	0.02	0.01	0.00
10	0.01	0.02	0.02	0.02	0.02	0.02	0.02	0.01	0.01	0.02	0.00	0.00	0.00	0.00	0.00	0.00	0.01	0.00	0.00	0.00	0.00	0.00	0.00	0.00	0.00
11	0.02	0.02	0.02	0.02	0.01	0.01	0.01	0.01	0.00	0.01	0.00	0.00	0.00	0.00	-0.01	0.00	0.00	0.00	-0.01	0.00	0.00	0.00	0.00	0.00	0.01
12	0.00	0.01	0.01	0.01	0.00	0.00	0.00	0.00	0.00	0.00	0.00	0.00	0.00	0.00	0.00	0.00	0.00	0.00	0.00	0.00	0.00	0.00	0.00	0.00	0.00
13	0.00	0.00	0.00	0.00	0.00	0.00	0.00	0.00	0.00	0.00	0.00	0.00	0.00	0.00	0.00	0.00	0.00	0.00	0.00	0.00	0.00	0.00	0.00	0.00	0.00
14	0.00	0.00	0.00	0.01	0.00	0.00	0.00	0.00	0.00	0.00	0.00	0.00	0.00	0.00	0.00	0.00	0.00	0.00	0.00	0.00	0.00	0.00	0.00	0.00	0.00
15	0.00	0.00	0.00	0.00	0.00	0.01	0.01	0.00	0.00	0.00	0.00	0.00	0.00	0.00	0.00	0.00	0.00	0.00	0.00	0.00	0.00	0.00	0.00	0.00	0.00

TABLE A3.--Field velocity data. Velocity ratios in the x direction on the x = 6 plane.

y Coordinate	z Coordinate 1	2	3	4	5	6	7	8	9	10	11	12	13	14	15	16	17	18	19	20	21	22	23	24	25
1							0.04	0.00	-0.02	-0.03	-0.02	-0.01	-0.01	-0.01	-0.01	-0.01	0.00	0.01	0.01	0.01	0.01	0.02	0.02	0.01	0.00
2	0.13	0.14	-0.03	0.01	0.18	0.03	0.00	-0.03	-0.04	-0.02	-0.01	-0.02	-0.01	-0.01	-0.01	0.00	0.01	0.00	0.01	0.01	0.01	0.02	0.02	0.01	-0.01
3	0.10	0.16	0.21	0.21	0.12	0.04	0.01	0.00	-0.01	0.00	0.00	-0.01	0.00	-0.01	0.00	0.00	0.00	0.00	0.01	0.01	0.01	0.01	0.02	0.01	0.00
4	0.08	0.12	0.16	0.15	0.11	0.07	0.03	0.02	0.00	0.00	0.00	-0.01	-0.02	-0.01	-0.01	0.00	0.01	0.00	0.00	0.01	0.01	0.01	0.02	0.01	0.01
5	0.07	0.10	0.13	0.12	0.10	0.09	0.09	0.08	0.02	0.03	0.02	0.01	0.00	0.00	0.00	0.01	0.02	0.00	0.01	0.01	0.01	0.01	0.01	0.01	0.00
6	0.04	0.08	0.08	0.07	0.05	0.04	0.03	0.02	0.01	0.01	0.00	0.00	0.00	0.00	0.00	0.00	0.01	0.00	0.00	0.02	0.01	0.01	0.01	0.01	0.00
7	0.05	0.05	0.08	0.05	0.05	0.05	0.04	0.02	0.02	0.02	0.01	0.01	0.00	0.01	0.01	0.01	0.01	0.00	0.01	0.02	0.01	0.01	0.01	0.01	0.00
8	0.04	0.05	0.07	0.08	0.05	0.04	0.07	0.05	0.04	0.03	0.02	0.02	0.01	0.01	0.01	0.02	0.02	0.02	0.02	0.02	0.03	0.03	0.02	0.02	0.01
9	0.02	0.03	0.03	0.04	0.04	0.03	0.04	0.04	0.04	0.02	0.02	0.01	0.01	0.01	0.02	0.02	0.02	0.02	0.02	0.02	0.02	0.02	0.01	0.01	0.01
10	0.01	0.01	0.01	0.02	0.02	0.01	0.01	0.01	0.01	0.01	0.01	0.00	0.00	0.00	0.00	0.00	0.00	0.00	0.00	0.00	0.00	0.00	0.00	0.01	0.01
11	0.01	0.00	0.00	0.01	0.01	0.01	0.01	0.00	0.00	0.00	0.00	-0.01	-0.01	-0.01	-0.01	-0.01	-0.01	-0.01	-0.01	0.00	-0.01	-0.01	-0.01	0.00	0.00
12	0.00	0.00	0.00	0.01	0.00	0.00	0.00	0.00	0.00	0.00	0.00	0.00	0.00	0.00	0.00	0.00	0.00	0.00	0.00	0.00	0.00	0.00	0.00	0.00	0.00
13	0.00	0.00	0.00	0.00	0.00	0.00	0.00	0.00	0.00	0.00	0.00	0.00	0.00	0.00	0.00	0.00	0.00	0.00	0.00	0.00	0.00	0.00	0.00	0.00	0.00
14	0.00	0.00	0.00	0.00	0.00	0.00	0.00	0.00	0.00	0.00	0.00	0.00	0.00	0.00	0.00	0.00	0.00	0.00	0.00	0.00	0.00	0.00	0.00	0.00	0.00
15	0.00	0.00	0.00	0.00	0.00	0.00	0.00	0.00	0.00	0.00	0.00	0.00	0.00	0.00	0.00	0.00	0.00	0.00	0.00	0.00	0.00	0.00	0.00	0.00	0.00

TABLE A4.--Field velocity data. Velocity ratios in the x direction on the x = 7 plane.

y Coordinate	z Coordinate 1	2	3	4	5	6	7	8	9	10	11	12	13	14	15	16	17	18	19	20	21	22	23	24	25
1							0.03	0.01	-0.03	-0.03	-0.03	-0.01	-0.01	-0.02	0.00	0.00	0.01	0.01	0.01	0.02	0.01	0.02	0.02	0.01	0.00
2	0.18	0.21	0.18	0.15	0.10	0.03	0.01	0.00	-0.03	-0.01	-0.02	-0.01	-0.01	0.00	0.00	0.00	0.01	0.01	0.01	0.01	0.01	0.02	0.02	0.02	0.00
3	0.11	0.13	0.16	0.16	0.10	0.05	0.03	0.01	-0.01	0.01	-0.02	0.00	0.01	0.01	0.00	0.01	0.01	0.01	0.01	0.01	0.01	0.02	0.02	0.02	0.00
4	0.07	0.08	0.12	0.10	0.09	0.04	0.03	-0.01	-0.01	-0.01	0.00	-0.01	-0.02	-0.01	-0.01	0.01	0.00	0.01	0.00	0.00	0.01	0.01	0.02	0.01	0.00
5	0.09	0.11	0.08	0.11	0.10	0.05	0.07	0.04	0.02	0.03	0.02	0.01	0.00	0.01	0.01	0.02	0.01	0.02	0.01	0.01	0.01	0.01	0.01	0.01	0.00
6	0.05	0.07	0.05	0.05	0.04	0.05	0.04	0.04	0.01	0.03	0.01	0.01	0.00	0.00	0.01	0.02	0.02	0.01	0.01	0.02	0.02	0.02	0.02	0.01	0.00
7	0.04	0.07	0.07	0.08	0.04	0.07	0.05	0.04	0.02	0.03	0.02	0.02	0.01	0.01	0.01	0.02	0.02	0.02	0.01	0.02	0.02	0.02	0.02	0.01	0.01
8	0.03	0.03	0.05	0.04	0.02	0.04	0.02	0.02	0.01	0.02	0.00	0.01	0.01	0.00	0.00	0.01	0.02	0.02	0.00	0.01	0.02	0.02	0.02	0.01	0.00
9	0.02	0.02	0.02	0.02	0.01	0.01	0.01	0.01	0.00	0.01	0.00	0.00	0.00	0.00	0.00	0.00	0.00	0.00	-0.01	0.01	0.00	0.00	0.00	0.00	0.00
10	0.01	0.01	0.01	0.01	0.00	0.00	0.01	0.00	0.00	0.00	0.00	-0.01	0.00	-0.01	0.00	-0.01	0.00	0.00	-0.01	-0.01	-0.01	-0.01	0.00	0.01	0.00
11	0.01	0.01	0.01	0.01	0.00	0.00	0.00	0.00	0.00	-0.01	-0.01	-0.01	-0.01	-0.01	-0.01	-0.01	-0.01	-0.01	-0.02	-0.01	-0.01	-0.01	0.00	0.01	0.00
12	0.00	0.01	0.00	0.01	0.00	0.00	0.00	0.00	0.00	0.00	0.00	0.00	0.00	0.00	0.00	0.00	0.00	0.00	-0.01	0.00	-0.01	-0.01	0.00	0.01	0.00
13	0.00	0.00	0.00	0.00	0.00	0.00	0.00	0.00	0.00	0.00	0.00	0.00	0.00	0.00	0.00	0.00	0.00	0.00	0.00	0.00	0.00	0.00	0.00	0.00	0.00
14	0.00	0.00	0.00	0.00	0.00	0.00	0.00	0.00	0.00	0.00	0.00	0.00	0.00	0.00	0.00	0.00	0.00	0.00	0.00	0.00	0.00	0.00	0.00	0.00	0.00
15	0.00	0.00	0.00	0.00	0.00	0.00	0.00	0.00	0.00	0.00	0.00	0.00	0.00	0.00	0.00	0.00	0.00	0.00	0.00	0.00	0.00	0.00	0.00	0.00	0.00

TABLE A5.--Field velocity data. Velocity ratios in the y direction on the x = 4 plane. Values in parentheses are within the gages top coundry layer.

y Coordinate	z Coordinate 1	2	3	4	5	6	7	8	9	10	11	12	13	14	15	16	17	18	19	20	21	22	23	24	25
1							0.22	0.15	0.08	0.05	0.05	0.05	0.03	0.04	0.03	0.02	0.03	0.03	0.03	0.02	0.01	0.01	0.01	0.00	0.00
2	(0.88)	(-9.45)	(-4.69)	(-6.60)	0.67	0.35	0.21	0.13	0.08	0.07	0.04	0.03	0.03	0.03	0.02	0.01	0.01	0.01	0.01	0.02	0.01	0.01	0.01	0.00	0.00
3	-0.41	-0.32	-0.12	0.19	0.24	0.22	0.15	0.11	0.07	0.09	0.05	0.05	0.03	0.04	0.03	0.02	0.02	0.02	0.03	0.02	0.01	0.01	0.01	0.01	0.01
4	-0.24	-0.20	-0.04	0.09	0.14	0.11	0.11	0.10	0.08	0.05	0.04	0.04	0.02	0.02	0.02	0.02	0.02	0.01	0.03	0.02	0.02	0.02	0.02	0.02	0.01
5	-0.16	-0.11	0.03	0.05	0.11	0.09	0.08	0.09	0.07	0.05	0.03	0.04	0.05	0.03	0.02	0.03	0.02	0.01	0.03	0.02	0.04	0.02	0.02	0.01	0.01
6	-0.10	-0.03	0.01	0.01	0.04	0.04	0.04	0.04	0.01	0.02	0.03	0.03	0.04	0.03	0.03	0.02	0.02	0.01	0.01	0.01	0.01	0.01	0.01	0.00	0.00
7	-0.01	-0.01	0.01	0.01	0.04	0.03	0.03	0.03	0.02	0.01	0.01	0.03	0.04	0.03	0.03	0.02	0.01	0.01	0.01	0.00	0.00	0.02	0.02	0.01	0.01
8	-0.01	-0.02	0.00	0.00	0.02	0.01	0.02	0.02	0.02	0.03	0.03	0.03	0.03	0.03	0.03	0.02	0.02	0.02	0.01	0.01	0.01	0.02	0.02	0.02	0.02
9	0.01	0.01	0.02	0.02	0.03	0.03	0.03	0.03	0.03	0.03	0.03	0.03	0.03	0.03	0.03	0.02	0.02	0.02	0.02	0.02	0.02	0.02	0.01	0.01	0.00
10	0.00	0.01	0.02	0.02	0.04	0.03	0.03	0.03	0.03	0.03	0.03	0.03	0.02	0.03	0.02	0.02	0.01	0.02	0.01	0.01	0.01	0.01	0.01	0.00	0.00
11	0.01	0.02	0.02	0.03	0.03	0.03	0.02	0.02	0.02	0.03	0.02	0.03	0.02	0.02	0.02	0.01	0.01	0.01	0.01	0.01	0.00	0.00	0.00	0.01	0.01
12	0.01	0.01	0.01	0.02	0.02	0.02	0.02	0.02	0.02	0.02	0.02	0.02	0.02	0.02	0.01	0.01	0.01	0.01	0.01	0.00	0.00	0.00	0.00	0.00	0.00
13	0.01	0.01	0.01	0.01	0.01	0.01	0.01	0.02	0.01	0.02	0.02	0.02	0.01	0.02	0.01	0.01	0.01	0.01	0.01	0.00	0.00	0.00	0.00	0.00	0.00
14	0.01	0.01	0.01	0.01	0.01	0.01	0.01	0.01	0.01	0.01	0.01	0.01	0.01	0.01	0.01	0.01	0.01	0.01	0.01	0.00	0.00	0.00	0.00	0.00	0.00
15	0.01	0.01	0.01	0.01	0.01	0.01	0.01	0.01	0.01	0.01	0.01	0.01	0.01	0.01	0.01	0.01	0.01	0.01	0.01	0.00	0.00	0.00	0.00	0.00	0.00

TABLE A6.--Field velocity data. Velocity ratios in the y direction on the x = 5 plane. Values in parentheses are within the gages top boundry layer.

y Coordinate	z Coordinate 1	2	3	4	5	6	7	8	9	10	11	12	13	14	15	16	17	18	19	20	21	22	23	24	25
1							0.18	0.11	0.07	0.07	0.04	0.04	0.03	0.03	0.02	0.01	0.01	0.00	0.01	0.00	0.00	0.01	0.01	0.00	0.00
2	-0.65	(10.82)	(-12.57)	(0.48)	0.40	0.27	0.15	0.10	0.07	0.05	0.01	0.02	0.03	0.02	0.01	0.01	0.01	0.02	0.01	0.01	0.01	0.01	0.00	0.01	0.01
3	-0.29	-0.30	-0.13	0.13	0.15	0.15	0.12	0.10	0.07	0.07	0.04	0.03	0.03	0.03	0.02	0.03	0.02	0.02	0.02	0.01	0.01	0.01	0.00	0.00	0.01
4	-0.22	-0.16	-0.02	0.08	0.11	0.11	0.10	0.09	0.04	0.04	0.03	0.03	0.03	0.04	0.03	0.01	0.01	0.02	0.02	0.01	0.02	0.01	0.01	0.01	0.01
5	-0.16	-0.08	0.05	0.04	0.08	0.09	0.09	0.08	0.05	0.04	0.03	0.05	0.03	0.04	0.03	0.03	0.03	0.02	0.02	0.01	0.02	0.02	0.02	0.01	0.00
6	-0.04	-0.02	0.00	0.02	0.03	0.04	0.04	0.04	0.03	0.02	0.03	0.02	0.03	0.04	0.03	0.02	0.02	0.02	0.02	0.01	0.00	0.01	0.02	0.01	0.00
7	-0.03	0.00	-0.01	0.01	0.02	0.03	0.02	0.02	0.04	0.02	0.02	0.02	0.02	0.02	0.02	0.01	0.01	0.01	0.01	0.00	0.00	0.00	0.00	0.00	0.00
8	-0.02	-0.03	0.01	0.03	0.03	0.02	0.02	0.03	0.03	0.03	0.02	0.02	0.01	0.02	0.02	0.02	0.02	0.02	0.02	0.02	0.01	0.01	0.01	0.01	0.01
9	0.01	0.02	0.04	0.05	0.04	0.03	0.03	0.03	0.04	0.03	0.03	0.03	0.03	0.03	0.03	0.02	0.02	0.02	0.02	0.02	0.02	0.02	0.02	0.01	0.01
10	0.02	0.02	0.03	0.04	0.03	0.04	0.04	0.04	0.04	0.04	0.04	0.03	0.03	0.04	0.03	0.03	0.02	0.02	0.02	0.02	0.02	0.02	0.01	0.01	0.02
11	0.01	0.02	0.03	0.03	0.04	0.03	0.03	0.03	0.03	0.02	0.03	0.03	0.03	0.03	0.02	0.02	0.02	0.02	0.02	0.01	0.01	0.01	0.01	0.01	0.01
12	0.01	0.01	0.01	0.02	0.01	0.02	0.02	0.02	0.01	0.01	0.02	0.02	0.01	0.02	0.01	0.01	0.01	0.01	0.01	0.00	0.00	0.00	0.00	0.00	0.00
13	0.01	0.01	0.01	0.01	0.01	0.01	0.01	0.02	0.01	0.01	0.01	0.01	0.01	0.01	0.01	0.01	0.01	0.01	0.00	0.00	0.00	0.00	0.00	0.00	0.00
14	0.01	0.01	0.01	0.01	0.01	0.01	0.01	0.01	0.01	0.01	0.01	0.01	0.01	0.01	0.01	0.01	0.01	0.01	0.00	0.00	0.00	0.00	0.00	0.00	0.00
15	0.01	0.01	0.01	0.01	0.01	0.01	0.01	0.01	0.01	0.01	0.01	0.01	0.01	0.01	0.01	0.01	0.01	0.01	0.00	0.00	0.00	0.00	0.00	0.00	0.00

TABLE A7.--Field velocity data. Velocity ratios in the y direction in the x = 6 plane.

y Coordinate	z Coordinate 1	2	3	4	5	6	7	8	9	10	11	12	13	14	15	16	17	18	19	20	21	22	23	24	25
1							0.13	0.09	0.07	0.04	0.03	0.03	0.03	0.02	0.01	0.00	0.00	0.01	0.01	0.00	0.00	0.00	0.00	0.00	0.00
2	-0.19	-0.37	-0.13	0.08	0.11	0.10	0.09	0.07	0.07	0.02	0.02	0.01	0.03	0.02	0.01	0.01	0.02	0.02	0.01	0.01	0.01	0.01	0.01	0.01	0.00
3	-0.25	-0.20	-0.03	0.08	0.09	0.09	0.08	0.05	0.03	0.02	0.03	0.02	0.03	0.04	0.01	0.01	0.03	0.02	0.01	0.01	0.01	0.01	0.01	0.00	0.00
4	-0.20	-0.13	0.04	0.05	0.07	0.07	0.07	0.05	0.04	0.03	0.02	0.03	0.02	0.01	0.02	0.01	0.01	0.01	0.01	0.01	0.02	0.01	0.01	0.01	0.00
5	-0.12	-0.04	0.01	0.03	0.05	0.08	0.07	0.05	0.03	0.02	0.03	0.03	0.02	0.02	0.01	0.01	0.01	0.01	0.01	0.01	0.02	0.02	0.02	0.01	0.00
6	-0.03	0.01	0.00	0.02	0.03	0.07	0.04	0.02	0.02	0.02	0.03	0.03	0.02	0.03	0.02	0.02	0.02	0.02	0.02	0.01	0.02	0.01	0.01	0.01	0.01
7	-0.01	-0.01	-0.01	0.00	0.02	0.03	0.02	0.02	0.01	0.03	0.01	0.02	0.02	0.03	0.02	0.02	0.03	0.02	0.03	0.02	0.01	0.02	0.02	0.02	0.01
8	-0.02	0.01	0.00	-0.01	0.03	0.02	0.02	0.02	0.03	0.02	0.01	0.03	0.02	0.03	0.03	0.03	0.03	0.02	0.03	0.02	0.02	0.03	0.02	0.02	0.02
9	0.01	0.02	0.02	0.03	0.04	0.05	0.03	0.03	0.03	0.04	0.04	0.03	0.03	0.03	0.03	0.03	0.03	0.03	0.03	0.02	0.02	0.02	0.02	0.01	0.01
10	0.02	0.03	0.03	0.04	0.04	0.04	0.04	0.04	0.04	0.04	0.04	0.03	0.04	0.03	0.03	0.03	0.03	0.03	0.02	0.02	0.02	0.02	0.02	0.02	0.02
11	0.02	0.02	0.03	0.03	0.04	0.04	0.04	0.04	0.03	0.03	0.03	0.03	0.03	0.03	0.03	0.03	0.02	0.02	0.02	0.01	0.01	0.01	0.01	0.01	0.01
12	0.01	0.01	0.01	0.01	0.02	0.02	0.02	0.02	0.02	0.02	0.02	0.02	0.02	0.02	0.01	0.01	0.01	0.01	0.01	0.00	0.00	0.00	0.00	0.00	0.00
13	0.01	0.01	0.01	0.01	0.01	0.01	0.01	0.01	0.01	0.02	0.02	0.01	0.01	0.01	0.01	0.01	0.01	0.01	0.01	0.00	0.00	0.00	0.00	0.00	0.00
14	0.01	0.01	0.01	0.01	0.01	0.01	0.02	0.01	0.01	0.01	0.01	0.01	0.01	0.01	0.01	0.01	0.01	0.00	0.00	0.00	0.00	0.00	0.00	0.00	0.00
15	0.01	0.01	0.01	0.01	0.01	0.01	0.01	0.01	0.01	0.01	0.01	0.01	0.01	0.01	0.01	0.01	0.00	0.00	0.00	0.00	0.00	0.00	0.00	0.00	0.00

TABLE A8.--Field velocity data. Velocity ratios in the y direction on the x = 7 plane.

y Coordinate	z Coordinate 1	2	3	4	5	6	7	8	9	10	11	12	13	14	15	16	17	18	19	20	21	22	23	24	25
1							0.08	0.07	0.05	0.03	0.02	-0.01	0.01	0.00	-0.01	-0.01	0.00	0.01	-0.01	-0.02	0.00	0.00	0.00	0.00	0.00
2	-0.23	-0.15	0.04	-0.03	0.04	0.08	0.05	0.07	0.02	0.03	0.02	0.02	0.01	0.02	0.00	0.00	0.01	0.01	0.01	0.00	0.01	0.01	0.01	0.01	0.00
3	-0.16	-0.12	-0.02	0.02	0.03	0.05	0.07	0.07	0.04	0.03	0.04	0.02	0.01	0.03	0.00	0.01	0.01	0.01	0.02	0.01	0.00	0.01	0.01	0.01	0.00
4	-0.15	-0.09	0.01	0.03	0.05	0.09	0.05	0.05	0.01	0.04	0.03	0.02	0.03	0.04	0.01	0.01	0.02	0.01	0.01	0.00	0.01	0.01	0.01	0.01	0.00
5	-0.02	0.00	0.01	0.03	0.05	0.04	0.03	0.04	0.03	0.03	0.02	0.03	0.02	0.04	0.01	0.02	0.02	0.02	0.02	0.02	0.02	0.02	0.02	0.02	0.02
6	0.00	0.00	0.01	0.01	0.03	0.03	0.05	0.04	0.02	0.02	0.03	0.01	0.02	0.03	0.01	0.02	0.02	0.01	0.02	0.00	0.02	0.02	0.02	0.02	0.02
7	-0.02	-0.02	0.01	0.02	0.01	0.02	0.03	0.03	0.01	0.01	0.02	0.00	0.03	0.03	0.02	0.02	0.03	0.03	0.03	0.01	0.02	0.02	0.01	0.00	0.01
8	-0.01	-0.01	-0.01	0.00	0.02	0.01	0.02	0.02	0.02	0.02	-0.02	0.02	0.02	0.01	0.01	0.01	0.01	0.01	0.01	0.00	0.00	0.00	0.00	0.01	0.01
9	0.01	0.01	0.02	0.02	0.03	0.02	0.02	0.03	0.02	0.02	0.03	0.02	0.02	0.02	0.01	0.01	0.01	0.01	0.01	0.00	0.00	0.00	0.01	0.01	0.01
10	0.01	0.01	0.01	0.01	0.02	0.03	0.02	0.02	0.02	0.02	0.02	0.02	0.02	0.02	0.02	0.01	0.01	0.02	0.01	0.00	0.00	0.00	0.00	0.01	0.01
11	0.01	0.01	0.02	0.02	0.02	0.02	0.02	0.02	0.01	0.02	0.02	0.02	0.02	0.01	0.02	0.01	0.01	0.01	0.01	0.00	0.00	0.00	0.00	0.01	0.00
12	0.01	0.01	0.01	0.01	0.02	0.02	0.02	0.01	0.01	0.02	0.02	0.01	0.02	0.02	0.02	0.01	0.01	0.01	0.01	0.00	0.00	0.00	0.00	0.00	0.00
13	0.01	0.01	0.01	0.01	0.01	0.01	0.01	0.01	0.01	0.01	0.01	0.01	0.02	0.01	0.01	0.01	0.01	0.01	0.00	0.00	0.00	0.00	0.00	0.00	0.00
14	0.01	0.01	0.01	0.01	0.01	0.01	0.01	0.01	0.01	0.01	0.01	0.01	0.01	0.01	0.01	0.01	0.01	0.00	0.00	0.00	0.00	0.00	0.00	0.00	0.00
15	0.01	0.01	0.01	0.01	0.01	0.01	0.01	0.01	0.01	0.01	0.01	0.01	0.01	0.01	0.01	0.01	0.01	0.01	0.00	0.00	0.00	0.00	0.00	0.00	0.00

TABLE A9.--Field velocity data. Velocity ratios in the negative z direction on the x = 4 plane. Values in parentheses are within the gages top boundary layer.

y Coordinate	z Coordinate 1	2	3	4	5	6	7	8	9	10	11	12	13	14	15	16	17	18	19	20	21	22	23	24	25
1							0.95	0.93	0.93	0.92	0.95	0.92	0.93	0.93	0.97	0.98	0.96	0.97	0.98	0.99	0.99	0.98	0.98	0.98	0.99
2	(21.42)	(6.00)	(2.79)	(3.82)	1.08	0.84	0.84	0.88	0.91	0.93	0.93	0.96	0.95	0.96	0.97	0.98	0.97	0.97	0.99	0.99	0.99	0.98	0.98	0.98	0.98
3	1.14	1.19	1.23	1.18	1.00	0.93	0.91	0.92	0.95	0.95	0.95	0.93	0.93	0.95	0.97	0.98	0.97	0.97	0.98	0.99	0.99	0.98	0.97	0.98	0.98
4	1.12	1.11	1.08	1.03	1.00	0.99	0.95	0.95	0.96	0.95	0.96	0.93	0.93	0.95	0.97	0.98	0.96	0.97	0.99	0.99	0.99	0.98	0.98	0.98	0.98
5	1.10	1.07	1.02	1.02	0.99	0.99	0.96	0.96	0.98	0.96	0.96	0.93	0.95	0.96	0.98	0.98	0.97	0.97	0.98	0.99	0.98	0.98	0.98	0.98	0.98
6	1.07	1.04	1.01	1.01	1.00	1.00	0.97	0.97	0.98	0.98	0.97	0.95	0.95	0.97	0.97	0.98	0.97	0.98	0.99	0.99	0.99	0.99	0.99	0.99	0.99
7	1.07	1.03	1.02	1.01	1.00	1.01	0.97	0.98	0.99	0.98	0.98	0.96	0.96	0.97	0.96	0.99	0.98	0.98	1.00	1.00	1.00	0.99	0.99	0.99	0.99
8	1.07	1.02	1.01	1.01	1.01	1.00	0.97	0.98	0.98	0.97	0.97	0.96	0.95	0.96	0.97	0.98	0.97	0.97	0.99	0.99	0.99	0.98	0.98	0.98	0.99
9	1.05	1.03	1.01	1.01	1.00	1.00	0.98	0.99	0.98	0.98	0.98	0.97	0.97	0.98	0.98	0.98	0.97	0.98	0.99	0.99	0.99	0.98	0.98	0.98	0.98
10	1.04	1.02	1.01	1.00	1.00	0.99	0.98	0.99	0.98	0.98	0.98	0.97	0.97	0.98	0.98	0.98	0.98	0.98	0.99	0.99	0.99	0.98	0.98	0.98	0.99
11	1.03	1.01	1.01	1.00	1.00	1.00	0.98	0.99	0.99	0.99	0.99	0.98	0.98	0.98	0.98	0.99	0.98	0.99	0.99	0.99	0.99	0.99	0.99	0.99	0.99
12	1.01	1.01	1.01	1.00	1.00	1.00	1.00	1.00	1.00	1.00	1.00	1.00	0.99	0.99	0.99	0.99	0.99	0.99	1.00	0.99	0.99	0.99	0.99	0.99	0.99
13	1.01	1.01	1.01	1.00	1.00	1.00	1.00	1.00	1.00	1.00	1.00	1.00	1.00	0.99	1.00	0.99	1.00	1.00	1.00	1.00	0.99	0.99	0.99	0.99	0.99
14	1.01	1.01	1.01	1.00	1.00	1.00	1.00	1.00	1.00	1.00	1.00	1.00	1.00	1.00	1.00	1.00	1.00	1.00	1.00	1.00	0.99	0.99	0.99	0.99	0.99
15	1.01	1.01	1.01	1.00	1.01	1.00	1.01	1.01	1.01	1.01	1.01	1.00	1.00	1.00	1.00	1.00	1.00	1.00	1.00	1.00	0.99	0.99	0.99	0.99	0.99

TABLE A10.--Field velocity data. Velocity ratios in the negative z direction on the x = 5 plane. Values in parentheses are within the gages top boundry layer.

y Coordinate	z Coordinate 1	2	3	4	5	6	7	8	9	10	11	12	13	14	15	16	17	18	19	20	21	22	23	24	25
1							0.98	0.98	0.95	0.91	0.93	0.93	0.95	0.93	0.96	0.97	0.97	0.98	0.96	0.97	0.98	0.98	0.98	0.96	0.98
2	1.07	(16.20)	(7.81)	(26.84)	1.09	0.89	0.96	0.89	0.92	0.92	0.93	0.96	0.95	0.96	0.96	0.97	0.97	0.97	0.98	0.98	0.98	0.98	0.98	0.98	0.96
3	1.12	1.15	1.22	1.09	1.03	0.96	0.91	0.92	0.93	0.95	0.95	0.93	0.93	0.96	0.96	0.97	0.98	0.98	0.98	0.97	0.98	0.98	0.98	0.98	0.97
4	1.11	1.09	1.07	1.02	1.01	0.98	0.95	0.95	0.96	0.96	0.96	0.96	0.93	0.95	0.97	0.97	0.97	0.97	0.98	0.99	0.98	0.98	0.98	0.98	0.98
5	1.10	1.07	1.02	1.01	1.00	1.00	0.97	0.97	0.97	0.97	0.96	0.96	0.95	0.95	0.97	0.97	0.97	0.97	0.98	0.98	0.99	0.98	0.97	0.98	0.97
6	1.07	1.03	1.02	1.01	1.01	1.01	0.97	0.98	0.98	0.98	0.98	0.96	0.96	0.96	0.97	0.98	0.98	0.97	0.99	0.99	0.99	0.98	0.98	0.98	0.98
7	1.07	1.03	1.02	1.01	1.01	1.00	0.98	0.99	0.99	0.98	0.99	0.97	0.97	0.98	0.98	0.99	0.99	0.99	1.00	1.00	0.99	0.99	0.98	0.99	0.99
8	1.05	1.02	1.00	1.00	1.00	1.00	0.97	0.98	0.97	0.97	0.97	0.95	0.95	0.96	0.96	0.97	0.98	0.98	0.99	0.98	0.99	0.98	0.97	0.97	0.98
9	1.04	1.02	1.00	1.00	1.00	0.99	0.98	0.98	0.98	0.98	0.98	0.97	0.97	0.97	0.98	0.98	0.98	0.98	0.98	0.99	0.99	0.98	0.98	0.98	0.98
10	1.03	1.01	1.00	1.00	0.99	0.99	0.98	0.98	0.98	0.98	0.98	0.97	0.98	0.98	0.98	0.98	0.99	0.98	0.98	0.99	0.98	0.98	0.98	0.98	0.98
11	1.03	1.02	1.01	1.00	1.00	1.00	0.99	0.99	0.99	0.99	0.99	0.98	0.99	0.99	0.98	0.99	0.99	0.99	0.99	0.99	1.00	0.99	0.99	0.99	0.99
12	1.01	1.01	1.01	1.00	1.00	1.00	1.00	1.00	1.00	1.00	1.00	0.99	0.99	1.00	0.99	0.99	1.00	0.99	0.99	0.99	0.99	0.99	0.99	0.99	0.99
13	1.01	1.01	1.01	1.00	1.00	1.00	1.00	1.00	1.00	1.00	1.00	1.00	1.00	1.00	1.00	1.00	1.00	1.00	1.00	0.99	0.99	0.99	0.99	0.99	0.99
14	1.01	1.01	1.01	1.01	1.01	1.00	1.00	1.00	1.00	1.00	1.00	1.00	1.00	1.00	1.00	1.00	1.00	1.00	1.00	1.00	0.99	0.99	0.99	0.99	0.99
15	1.01	1.01	1.01	1.01	1.01	1.00	1.01	1.01	1.01	1.01	1.01	1.00	1.00	1.00	1.00	1.00	1.00	1.00	1.00	1.00	1.00	0.99	0.99	0.99	0.99

TABLE A11.--Field velocity data. Velocity ratios in the negative z direction on the x = 0 plane.

y Coordinate	z Coordinate 1	2	3	4	5	6	7	8	9	10	11	12	13	14	15	16	17	18	19	20	21	22	23	24	25
1							1.04	1.01	0.96	0.91	0.93	0.93	0.92	0.93	0.96	0.96	0.96	0.98	0.98	0.98	0.98	0.98	0.97	0.97	0.98
2	1.15	1.23	1.23	1.19	1.05	0.96	0.90	0.90	0.93	0.92	0.93	0.95	0.95	0.93	0.97	0.97	0.97	0.98	0.98	0.99	0.98	0.98	0.97	0.97	0.97
3	1.13	1.10	1.08	1.04	1.03	0.99	0.92	0.93	0.95	0.93	0.95	0.95	0.95	0.93	0.97	0.97	0.96	0.97	0.97	0.99	0.98	0.97	0.96	0.97	0.97
4	1.11	1.07	1.02	1.01	1.01	0.99	0.96	0.95	0.96	0.96	0.95	0.96	0.96	0.93	0.97	0.97	0.96	0.98	0.98	0.99	0.98	0.97	0.97	0.97	0.97
5	1.09	1.04	1.01	1.02	1.00	1.00	0.97	0.96	0.97	0.96	0.95	0.96	0.96	0.95	0.98	0.98	0.97	0.98	0.98	0.99	0.98	0.97	0.97	0.97	0.98
6	1.05	1.03	1.01	1.02	1.02	1.00	0.98	0.98	0.96	0.97	0.96	0.96	0.96	0.96	0.98	0.98	0.97	0.98	0.99	0.99	0.98	0.98	0.97	0.98	0.98
7	1.07	1.03	1.01	1.02	1.01	1.01	0.99	0.98	0.98	0.97	0.97	0.98	0.97	0.96	0.99	0.98	0.97	0.99	0.99	1.00	0.99	0.98	0.98	0.98	0.98
8	1.04	1.01	1.00	1.00	1.00	0.99	0.97	0.97	0.97	0.96	0.96	0.96	0.95	0.95	0.96	0.96	0.96	0.97	0.98	0.98	0.98	0.97	0.97	0.97	0.98
9	1.04	1.02	1.00	1.00	1.00	0.99	0.98	0.98	0.98	0.98	0.98	0.98	0.97	0.98	0.98	0.97	0.98	0.98	0.98	0.99	0.99	0.98	0.98	0.98	0.97
10	1.03	1.01	1.00	1.00	1.00	0.99	0.98	0.99	0.99	0.98	0.98	0.98	0.98	0.98	0.98	0.97	0.98	0.98	0.98	0.99	0.99	0.98	0.98	0.98	0.98
11	1.03	1.02	1.01	1.01	1.01	1.00	0.99	0.99	0.99	0.99	0.99	0.98	0.99	0.99	0.99	0.99	0.99	0.99	0.99	0.99	0.99	0.99	0.99	0.99	0.99
12	1.01	1.01	1.01	1.01	1.00	1.00	1.00	1.00	1.00	1.00	1.00	1.00	0.99	0.99	0.99	0.99	1.00	0.99	0.99	1.00	0.99	0.99	0.99	0.99	0.99
13	1.01	1.01	1.01	1.01	1.00	1.00	1.00	1.00	1.00	1.00	1.00	1.00	1.00	1.00	0.99	1.00	1.00	1.00	1.00	1.00	1.00	0.99	0.99	0.99	0.99
14	1.01	1.01	1.01	1.01	1.00	1.00	1.00	1.00	1.00	1.00	1.00	1.00	1.00	1.00	1.00	1.00	1.00	1.00	1.00	1.00	0.99	0.99	0.99	0.99	0.99
15	1.01	1.01	1.01	1.01	1.01	1.00	1.00	1.01	1.01	1.01	1.01	1.01	1.00	1.00	1.00	1.00	1.00	1.00	1.00	1.00	1.00	0.99	0.99	0.99	0.99

TABLE A12.--Field velocity data. Velocity ratios in the negative z direction on the x = 7 plane.

y Coordinate	z Coordinate 1	2	3	4	5	6	7	8	9	10	11	12	13	14	15	16	17	18	19	20	21	22	23	24	25
1							1.10	1.03	0.97	0.92	0.92	0.92	0.93	0.93	0.96	0.98	0.96	0.97	0.97	0.98	0.98	0.97	0.96	0.97	0.98
2	1.11	1.10	1.04	1.08	1.01	0.98	0.92	0.91	0.95	0.93	0.93	0.93	0.93	0.96	0.96	0.97	0.96	0.97	0.97	0.98	0.98	0.97	0.97	0.97	0.97
3	1.10	1.08	1.05	1.03	1.03	1.00	0.93	0.92	0.95	0.95	0.93	0.95	0.95	0.96	0.97	0.98	0.97	0.98	0.97	0.98	0.98	0.97	0.97	0.97	0.97
4	1.09	1.05	1.02	1.00	1.01	1.00	0.95	0.95	0.98	0.95	0.93	0.96	0.93	0.96	0.97	0.98	0.96	0.98	0.97	0.98	0.98	0.98	0.97	0.97	0.97
5	1.05	1.03	1.02	1.01	1.00	1.00	0.97	0.97	0.97	0.96	0.96	0.96	0.93	0.97	0.98	0.98	0.96	0.97	0.97	0.98	0.97	0.97	0.96	0.97	0.97
6	1.04	1.03	1.01	1.01	1.01	1.01	0.98	0.97	0.96	0.96	0.96	0.97	0.96	0.97	0.98	0.98	0.97	0.97	0.98	0.99	0.98	0.97	0.97	0.97	0.98
7	1.05	1.03	1.01	1.01	1.02	1.01	0.98	0.97	1.00	0.97	0.97	0.97	0.96	0.97	0.98	0.98	0.97	0.98	0.98	0.99	0.98	0.97	0.97	0.98	0.99
8	1.04	1.02	1.00	1.00	1.01	1.00	0.98	0.97	0.99	0.97	0.97	0.97	0.96	0.98	0.97	0.97	0.97	0.99	0.99	0.99	0.98	0.97	0.97	0.97	0.98
9	1.03	1.02	1.00	1.00	1.00	0.99	0.98	0.98	0.98	0.98	0.98	0.98	0.97	0.98	0.98	0.98	0.99	0.98	0.98	0.99	0.99	0.98	0.98	0.98	0.98
10	1.03	1.01	1.00	1.00	1.00	1.00	0.98	0.98	0.98	0.98	0.98	0.97	0.97	0.98	0.98	0.98	0.98	0.98	0.99	0.99	0.99	0.98	0.98	0.98	0.98
11	1.03	1.01	1.01	1.00	1.00	1.00	0.99	0.99	0.99	0.99	0.98	0.98	0.98	0.98	0.98	0.98	0.99	0.99	0.99	0.99	0.99	0.98	0.98	0.99	0.99
12	1.01	1.01	1.01	1.01	1.00	1.00	1.00	1.00	1.00	1.00	1.00	1.00	0.99	1.00	1.00	1.00	1.00	1.00	1.00	1.00	0.99	0.99	0.99	0.99	0.99
13	1.01	1.01	1.01	1.00	1.00	1.00	1.00	1.00	1.00	1.00	1.00	1.00	1.00	1.00	1.00	1.00	1.00	1.00	1.00	1.00	0.99	0.99	0.99	0.99	0.99
14	1.01	1.01	1.01	1.01	1.00	1.00	1.00	1.00	1.00	1.00	1.00	1.00	1.00	1.00	1.00	1.00	1.00	1.00	1.00	1.00	1.00	0.99	0.99	0.99	0.99
15	1.01	1.01	1.01	1.01	1.01	1.01	1.00	1.01	1.00	1.01	1.00	1.00	1.00	1.00	1.00	1.00	1.00	1.00	1.00	1.00	1.00	0.99	0.99	0.99	0.99

APPENDIX B

```
      PROGRAM TRANS

C           TO CONVERT ANEMOMETER BRIDGE VOLTAGES FROM A THREE SENSOR
C           PROBE TO VELOCITY COMPONENTS ALONG THE MODEL AXIS SYSTEM
      DIMENSION VAX(4,15,25), VAY(4,15,25), VAZ(4,15,25),
     1  IVAX(4,15,25), IVAY(4,15,25), IVAZ(4,15,25)
      RAD = 57.2957795
      PIE = 3.14159265
      NA1 = 3HVX1
      NA2 = 3HVY2
      NA3 = 3HVZ3
C           SUBSENSOR TO MODEL AXIS ANGLES
      AXXPP = 90.0
      AXYPP = 45.0
      AXZPP = 135.0
      AYXPP = RAD * ACOSF(SQRTF(2./3.))
      AYYPP = RAD * ACOSF(-SQRTF(1./6.))
      AYZPP = AYYPP
      AZXPP = RAD * ACOSF(SQRTF(1./3.))
      AZYPP = AZZPP = AZXPP
      SINXXPP = 1.0
      SINXYPP = SQRTF(1./2.)
      SINXZPP = SINXYPP
      SINYXPP = SINF(AYXPP/RAD)
      SINYYPP = SINF(AYYPP/RAD)
      SINYZPP = SINYYPP
      SINZXPP = SINF(AZXPP/RAD)
      SINZYPP = SINZZPP = SINZXPP
      COSXXPP = 0.0
      COSXYPP = SQRTF(1./2.)
      COSXZPP = -COSXYPP
      COSYXPP = SQRTF(2./3.)
      COSYYPP = -SQRTF(1./6.)
      COSYZPP = COSYYPP
      COSZXPP = SQRTF(1./3.)
      COSZYPP = COSZZPP = COSZXPP
C           READ IN SENSOR TO OPPOSITE SENSOR PLANE ANGLE AND ANGLED FLOW
C           COEFFICIENT
C           FIND SENSOR-SENSOR ANGLE
      READ 100, AVOXP, AK
  100 FORMAT (2F6.2)
      ALPHA = 89.99
   50 ALPHA = ALPHA + 0.01
      AB = SINF(ALPHA/RAD)/SINF((180.-ALPHA)/(2.*RAD))
      BR = AB / (2.*SINF(60./RAD))
      SR = AB / (2.*TANF(60./RAD))
      H = SQRTF(1. - BR*BR)
      AVOXP1 = RAD * (ATANF(BR/H) + ATANF(SR/H))
      IF (AVOXP - AVOXP1) 51,50,50
   51 CONTINUE
C           FIND SENSOR TO MODEL AXIS ANGLES
      DY1PZ1P = SINF(ALPHA/RAD)/SINF((180.-ALPHA)/(2.*RAD))
      DX1PY1P = DX1PZ1P = DY1PZ1P
      DX1PZ1 = .5 * DY1PZ1P / SINF(60./RAD)
      DY1PZ1 = DZ1PZ1 = DX1PZ1
      AZXP = RAD * ASINF(DX1PZ1)
      AZYP = AZZP = AZXP
      SINZXP = DX1PZ1
      SINZYP = SINZZP = SINZXP
      COSZXP = COSF(ASINF(DX1PZ1))
      COSZYP = COSZZP = COSZXP
```

```
      AXXP = 90.0
      SINXXP = 1.0
      COSXXP = 0.0
      AYXP = 90. - AZXP
      SINYXP = SINF(AYXP/RAD)
      COSYXP = COSF(AYXP/RAD)
      DVZ1 = .5 * DY1PZ1P / TANF(60./RAD)
      DUY1P = DWX1 = DVZ1
      AYYP = 90. + RAD * SINF(DUY1P)
      AYZP = AYYP
      SINYYP = SINF(AYYP/RAD)
      SINYZP = SINYYP
      COSYYP = COSF(AYYP/RAD)
      COSYZP = COSYYP
      DOZ1 = SQRTF(1. - DX1PZ1 * DX1PZ1)
      DUX1 = DOZ1
      DX1Y1P = SQRTF(DUX1 * DUX1 + DUY1P * DUY1P)
      AXYP = RAD * ASINF(DX1Y1P)
      SINXYP = DX1Y1P
      COSXYP = COSF(AXYP/RAD)
      AXZP = 180.0 - AXYP
      SINXZP = SINF(AXZP / RAD)
      COSXZP = COSF(AXZP / RAD)
C        FIND SUBSENSOR TO SENSOR ANGLES
      AXPXPP = RAD*ACOSF(COSXXP*COSXXPP+COSYXP*COSYXPP+COSZXP*COSZXPP)
      AXPYPP = RAD*ACOSF(COSXXP*COSXYPP+COSYXP*COSYYPP+COSZXP*COSZYPP)
      AXPZPP = RAD*ACOSF(COSXXP*COSXZPP+COSYXP*COSYZPP+COSZXP*COSZZPP)
      AYPXPP = RAD*ACOSF(COSXYP*COSXXPP+COSYYP*COSYXPP+COSZYP*COSZXPP)
      AYPYPP = RAD*ACOSF(COSXYP*COSXYPP+COSYYP*COSYYPP+COSZYP*COSZYPP)
      AYPZPP = RAD*ACOSF(COSXYP*COSXZPP+COSYYP*COSYZPP+COSZYP*COSZZPP)
      AZPXPP = RAD*ACOSF(COSXZP*COSXXPP+COSYZP*COSYXPP+COSZZP*COSZXPP)
      AZPYPP = RAD*ACOSF(COSXZP*COSXYPP+COSYZP*COSYYPP+COSZZP*COSZYPP)
      AZPZPP = RAD*ACOSF(COSXZP*COSXZPP+COSYZP*COSYZPP+COSZZP*COSZZPP)
      SINXPXPP = SINF(AXPXPP/RAD)
      SINXPYPP = SINF(AXPYPP/RAD)
      SINXPZPP = SINF(AXPZPP/RAD)
      SINYPXPP = SINF(AYPXPP/RAD)
      SINYPYPP = SINF(AYPYPP/RAD)
      SINYPZPP = SINF(AYPZPP/RAD)
      SINZPXPP = SINF(AZPXPP/RAD)
      SINZPYPP = SINF(AZPYPP/RAD)
      SINZPZPP = SINF(AZPZPP/RAD)
      COSXPXPP = COSF(AXPXPP/RAD)
      COSXPYPP = COSF(AXPYPP/RAD)
      COSXPZPP = COSF(AXPZPP/RAD)
      COSYPXPP = COSF(AYPXPP/RAD)
      COSYPYPP = COSF(AYPYPP/RAD)
      COSYPZPP = COSF(AYPZPP/RAD)
      COSZPXPP = COSF(AZPXPP/RAD)
      COSZPYPP = COSF(AZPYPP/RAD)
      COSZPZPP = COSF(AZPZPP/RAD)
C        FIND DETERMINATE AND COFACTOR VALUES FOR CONVERSION OF SENSED
C        VELOCITIES TO MODEL AXIS COMPONENT VELOCITIES
      A11 = SINXPXPP**2
      A12 = SINXPYPP**2
      A13 = SINXPZPP**2
      A21 = SINYPXPP**2
      A22 = SINYPYPP**2
      A23 = SINYPZPP**2
      A31 = SINZPXPP**2
      A32 = SINZPYPP**2
      A33 = SINZPZPP**2
```

```
      DENOM = A11*A22*A33+A12*A23*A31+A13*A21*A32-A13*A22*A31-
     1A12*A21*A33-A11*A23*A32
      C11 = A22*A33 - A23*A32
      C12 = A21*A33 - A23*A31
      C13 = A21*A32 - A22*A31
      C21 = A12*A33 - A13*A32
      C22 = A11*A33 - A13*A31
      C23 = A11*A32 - A12*A31
      C31 = A12*A23 - A13*A22
      C32 = A11*A23 - A13*A21
      C33 = A11*A22 - A12*A21
C        PRINT OUT ANGLES, SINES AND COSINES FOR PROGRAMMING CHECK
      PRINT 200, ALPHA,AXXPP,AXYPP,AXZPP,AYXPP,AYYPP,AYZPP,AZXPP,AZYPP,
     1AZZPP,SINXXPP,SINXYPP,SINXZPP,SINYXPP,SINYYPP,SINYZPP,SINZXPP,
     2SINZYPP,SINZZPP,COSXXPP,COSXYPP,COSXZPP,COSYXPP,COSYYPP,COSYZPP,
     3COSZXPP,COSZYPP,COSZZPP
  200 FORMAT (1H1,7X,8HALPHA =  F5.1//3(3(15X,3F10.5/)/))
      PRINT 201, AXXP,AXYP,AXZP,AYXP,AYYP,AYZP,AZXP,AZYP,AZZP,SINXXP,
     1SINXYP,SINXZP,SINYXP,SINYYP,SINYZP,SINZXP,SINZYP,SINZZP,COSXXP,
     2COSXYP,COSXZP,COSYXP,COSYYP,COSYZP,COSZXP,COSZYP,COSZZP
  201 FORMAT (  ///3(3(15X,3F10.5/)/))
      PRINT 201,AXPXPP,AXPYPP,AXPZPP,AYPXPP,AYPYPP,AYPZPP,AZPXPP,AZPYPP,
     1AZPZPP,SINXPXPP,SINXPYPP,SINXPZPP,SINYPXPP,SINYPYPP,SINYPZPP,
     2SINZPXPP,SINZPYPP,SINZPZPP,COSXPXPP,COSXPYPP,COSXPZPP,COSYPXPP,
     3COSYPYPP,COSYPZPP,COSZPXPP,COSZPYPP,COSZPZPP
      PRINT 202,DENOM,A11,A12,A13,A21,A22,A23,A31,A32,A33,C11,C12,C13,
     1C21,C22,C23,C31,C32,C33
  202 FORMAT (/// 15X,F10.5//3(3(15X,3F10.5/)/)1H1)
C        READ IN FIRST DATA CARD AND JUMP TO DATA CONVERSION ROUTINE
      READ 101, NUM, IX, IY, IZ, VNXP,VNYP,VNZP
  101 FORMAT (5X,I1,1X, 3(6X,I2),1X, 3(5X,F3.1))
      GO TO 12
C        READ IN ADDITIONAL DATA CARDS
C        IF EOF, PRINT OUT AND TERMINATE
C        IF NEW MODEL PRINT OUT AND CONTINUE DATA CONVERSION
   10 READ 101, NM, IX, IY, IZ, VNXP, VNYP, VNZP
      IF (EOF,60) 20,11
   11 IF (NUM-NM) 21,12,21
   12 VAXPP2 = C11*VNXP**2 - C21*VNYP**2 + C31*VNZP**2
      VAYPP2 =-C12*VNXP**2 + C22*VNYP**2 - C32*VNZP**2
      VAZPP2 = C13*VNXP**2 - C23*VNYP**2 + C33*VNZP**2
      VAXPP = SQRTF(ABSF(VAXPP2))
      VAYPP = SQRTF(ABSF(VAYPP2))
      VAZPP = SQRTF(ABSF(VAZPP2))
      VXP = COSXXPP*VAXPP + COSXYPP*VAYPP + COSXZPP*VAZPP
      VYP = COSYXPP*VAXPP + COSYYPP*VAYPP + COSYZPP*VAZPP
      VZP = COSZXPP*VAXPP + COSZYPP*VAYPP + COSZZPP*VAZPP
      DENM = SQRTF(VXP*VXP + VYP*VYP + VZP*VZP)
      THE1 = ACOSF((COSXXPP*VXP + COSYXPP*VYP + COSZXPP*VZP)/DENM)
      THE2 = ACOSF((COSXYPP*VXP + COSYYPP*VYP + COSZYPP*VZP)/DENM)
      THE3 = ACOSF((COSXZPP*VXP + COSYZPP*VYP + COSZZPP*VZP)/DENM)
      V1P = SQRTF(SINF(THE1)**2 + AK*AK*COSF(THE1)**2)*VNXP
      V2P = SQRTF(SINF(THE2)**2 + AK*AK*COSF(THE2)**2)*VNYP
      V3P = SQRTF(SINF(THE3)**2 + AK*AK*COSF(THE3)**2)*VNZP
      VB1P = SQRTF((V3P*V3P + V2P*V2P - V1P*V1P)/2.)
      VB2P = SQRTF((V3P*V3P + V1P*V1P - V2P*V2P)/2.)
      VB3P = SQRTF((V2P*V2P + V1P*V1P - V3P*V3P)/2.)
      VAX(IX,IY,IZ) = COSXXPP*VB1P + COSXYPP*VB2P + COSXZPP*VB3P
      VAY(IX,IY,IZ) = COSYXPP*VB1P + COSYYPP*VB2P + COSYZPP*VB3P
      VAZ(IX,IY,IZ) = COSZXPP*VB1P + COSZYPP*VB2P + COSZZPP*VB3P
      IVAX(IX,IY,IZ) = 100. * VAX(IX,IY,IZ)
      IVAY(IX,IY,IZ) = 100. * VAY(IX,IY,IZ)
```

```
      IVAZ(IX,IY,IZ) = 100. * VAZ(IX,IY,IZ)
C        RETURN TO READ ANOTHER DATA CARD
      GO TO 10
C       IF EOF COME HERE
   20 NO = 1
      GO TO 22
C       IF NEW MODEL COME HERE
   21 NO = 0
      NUM = NM
   22 PRINT 204, (I,(((VAX(I,J,K),K=1,25),(VAY(I,J,K),K=1,25),(VAZ(I,
     1J,K,),K=1,25)),J=1,15),I=1,4)
  204 FORMAT (4(1H1,4H X = I2//15(6H V(X)  25F5.1/6H V(Y)  25F5.1/
     1   6H V(Z)  25F5.1//)))
      DO 24 I = 1,4
      DO 24 J = 1,15
      PUNCH 206, I,J,NA1, (K,IVAX(I,J,K),K= 1, 7)
      PUNCH 206, I,J,NA1, (K,IVAX(I,J,K),K= 8,13)
      PUNCH 206, I,J,NA1, (K,IVAX(I,J,K),K=14,19)
      PUNCH 206, I,J,NA1, (K,IVAX(I,J,K),K=20,25)
      PUNCH 206, I,J,NA2, (K,IVAY(I,J,K),K= 1, 7)
      PUNCH 206, I,J,NA2, (K,IVAY(I,J,K),K= 8,13)
      PUNCH 206, I,J,NA2, (K,IVAY(I,J,K),K=14,19)
      PUNCH 206, I,J,NA2, (K,IVAY(I,J,K),K=20,25)
      PUNCH 206, I,J,NA3, (K,IVAZ(I,J,K),K= 1, 7)
      PUNCH 206, I,J,NA3, (K,IVAZ(I,J,K),K= 8,13)
      PUNCH 206, I,J,NA3, (K,IVAZ(I,J,K),K=14,19)
   24 PUNCH 206, I,J,NA3, (K,IVAZ(I,J,K),K=20,25)
  206 FORMAT (I2,I3,1X,A3,1X,7(I2,I8))
      DO 23 I = 1,4
      DO 23 J = 1,15
      DO 23 K = 1,25
      IVAX(I,J,K) = IVAY(I,J,K) = IVAZ(I,J,K) = 0
   23 VAX(I,J,K) = VAY(I,J,K) = VAZ(I,J,K) = 0.0
      IF (NO) 12,12,30
   30 PRINT 205
  205 FORMAT (1H1)
      END
```

```
      PROGRAM CORRECT1

C          PROGRAM TO CORRECT FOR PROBE MISALIGNMENT
      DIMENSION IZ(7), DATA(7), VX(5,15,25), VY(5,15,25), VZ(5,15,25),
     1  VXC(5,15,25), VYC(5,15,25), VZC(5,15,25), VFLD(2,25)
      NA1 = 3HVX1
      NA2 = 3HVY2
      NA3 = 3HVZ3
C          RETURN HERE FOR RERUN
    9 DO 10 I = 1,5
      DO 10 J = 1,15
      DO 10 K = 1,25
      VX(I,J,K) = VY(I,J,K) = VZ(I,J,K) = 0.0
   10 VXC(I,J,K) = VYC(I,J,K) = VZC(I,J,K) = 0.0
      DO 11 J = 1,25
   11 VFLD (1,J) = VFLD(2,J) = 0.0
C          READ IN ARRAY SIZE LIMITS
C          IF NO MORE DATA GO TO END (EOF)
      READ 1000, IXLMT,IYLMT,IZLMT
 1000 FORMAT (3I2)
      IF (EOF,60) 90,20
C          READ IN MODEL FIELD DATA
   20 READ 1001, IX,IY,IDR,(IZ(I),DATA(I),I=1,7)
 1001 FORMAT (I2,I3,3X,I1,1X,7(I2,F8.2))
C          IF END OF MODEL FIELD DATA  GO TO 30
      IF (IX-8) 21,21,30
   21 IF (IDR-2) 22,24,26
   22 DO 23 I = 1,7
      IF (IZ(I)) 20,20,23
   23 VX(IX,IY,IZ(I)) = DATA(I)
      GO TO 20
   24 DO 25 I = 1,7
      IF (IZ(I)) 20,20,25
   25 VY(IX,IY,IZ(I)) = DATA(I)
      GO TO 20
   26 DO 27 I = 1,7
      IF (IZ(I)) 20,20,27
   27 VZ(IX,IY,IZ(I)) = DATA(I)
      GO TO 20
C          READ IN CORRECTION FIELD DATA
   30 READ 1001, IX,IY,IDR,(IZ(I),DATA(I),I=1,7)
C          IF END OF CORRECTION FIELD DATA  GO TO 40
      IF (IX-8) 31,31,40
   31 IF (IDR-2) 32,34,36
   32 DO 33 I = 1,7
      IF (IZ(I)) 30,30,33
   33 VXC(IX,IY,IZ(I)) = DATA(I)
      GO TO 30
   34 DO 35 I = 1,7
      IF (IZ(I)) 30,30,35
   35 VYC(IX,IY,IZ(I)) = DATA(I)
      GO TO 30
   36 DO 37 I = 1,7
      IF (IZ(I)) 30,30,37
   37 VZC(IX,IY,IZ(I)) = DATA(I)
      GO TO 30
C          PRINT OUT FIELD DATA AS PROGRAM AND DATA CHECK
   40 PRINT 2000, (I,(((VX(I,J,K),K=1,25),(VY(I,J,K),K=1,25),(VZ(I,J,
     1K),K=1,25)),J=1,15),I=1,IXLMT)
 2000 FORMAT (5(1H1,4H X = I2//15(6H V(X)  25F5.1/6H V(Y)  25F5.1/
     1  6H V(Z)  25F5.1//)))
```

```
      PRINT 2000, (I,(((VXC(I,J,K),K=1,25),(VYC(I,J,K),K=1,25),
     1  (VZC(I,J,K),K=1,25)),J=1,15),I=1,IXLMT)
C         READ IN VFLD DATA (PRANDTL TUBE MEASUREMENTS)
C               IMOD = 1 - MODEL DATA
C               IMOD = 2 - CHECK DATA
C               JZ - Z PLANE
   41 READ 1002, IMOD,JZ,VFL
 1002 FORMAT (2I3,F6.2)
C         AT END OF VFLD DATA  GO TO 50
      IF (IMOD-8) 42,42,50
   42 VFLD(IMOD,JZ) = VEL
      GO TO 41
C         INTERPOLATE TO FILL IN CORRECTION FIELD ARRAYS IN Z PLANES
   50 K = 1
   51 DO 52 I = 2,3
      DO 52 J = 1,IYLMT
      IA = I - 1
      VXC(I,J,K) = VXC(1,J,K) + (VXC(4,J,K)-VXC(1,J,K))*IA/3.
      VYC(I,J,K) = VYC(1,J,K) + (VYC(4,J,K)-VYC(1,J,K))*IA/3.
   52 VZC(I,J,K) = VZC(1,J,K) + (VZC(4,J,K)-VZC(1,J,K))*IA/3.
      IF (K-12) 53,54,55
   53 K = 12
      GO TO 51
   54 K = 25
      GO TO 51
   55 CONTINUE
      DO 67 I = 1,IXLMT
      DO 67 J = 1,IYLMT
      CALL CURFT3 (1.,12.,25.,VXC(I,J,1),VXC(I,J,12),VXC(I,J,25),A,B,C)
      DO 61 K = 2,11
      AK = K
   61 VXC(I,J,K) = A*AK*AK + B*AK + C
      DO 62 K = 13,24
      AK = K
   62 VXC(I,J,K) = A*AK*AK + B*AK + C
      CALL CURFT3 (1.,12.,25.,VYC(I,J,1),VYC(I,J,12),VYC(I,J,25),A,B,C)
      DO 63 K = 2,11
      AK = K
   63 VYC(I,J,K) = A*AK*AK + B*AK + C
      DO 64 K = 13,24
      AK = K
   64 VYC(I,J,K) = A*AK*AK + B*AK + C
      CALL CURFT3 (1.,12.,25.,VZC(I,J,1),VZC(I,J,12),VZC(I,J,25),A,B,C)
      DO 65 K = 2,11
      AK = K
   65 VZC(I,J,K) = A*AK*AK + B*AK + C
      DO 66 K = 13,24
      AK = K
   66 VZC(I,J,K) = A*AK*AK + B*AK + C
   67 CONTINUE
C         INTERPOLATE TO FILLIN FIELD DATA ARRAY AT Z = 22, 24
      DO 68 I = 1,IXLMT
      DO 68 J = 1,IYLMT
      CALL CURFT3 (21.,23.,25.,VX(I,J,21),VX(I,J,23),VX(I,J,25),A,B,C)
      VX(I,J,22) = A*22.*22. + B*22. + C
      VX(I,J,24) = A*24.*24. + B*24. + C
      CALL CURFT3 (21.,23.,25.,VY(I,J,21),VY(I,J,23),VY(I,J,25),A,B,C)
      VY(I,J,22) = A*22.*22. + B*22. + C
      VY(I,J,24) = A*24.*24. + B*24. + C
      CALL CURFT3 (21.,23.,25.,VZ(I,J,21),VZ(I,J,23),VZ(I,J,25),A,B,C)
      VZ(I,J,22) = A*22.*22. + B*22. + C
   68 VZ(I,J,24) = A*24.*24. + B*24. + C
```

```
C         PRINT OUT FILLED IN MODEL AND CORRECTION ARRAYS
      PRINT 2000, (I,(((VX(I,J,K),K=1,25),(VY(I,J,K),K=1,25),(VZ(I,J,
     1K),K=1,25)),J=1,15),I=1,IXLMT)
      PRINT 2000, (I,(((VXC(I,J,K),K=1,25),(VYC(I,J,K),K=1,25),
     1   (VZC(I,J,K),K=1,25)),J=1,15),I=1,IXLMT)
C         CONVERT MODEL FIELD VELOCITY ARRAYS TO VELOCITY RATIO ARRAYS
      DO 72 I = 1,IXLMT
      DO 72 J = 1,IYLMT
      DO 72 K = 1,IZLMT
      VX(I,J,K) = VX(I,J,K) / VFLD(1,K)
      VY(I,J,K) = VY(I,J,K) / VFLD(1,K)
   72 VZ(I,J,K) = VZ(I,J,K) / VFLD(1,K)
C         CONVERT CORRECTION VELOCITY FIELD ARRAYS TO VEL RATIO ARRAYS
      DO 74 I = 1,IXLMT
      DO 74 J = 1,IYLMT
      DO 74 K = 1,IZLMT
      VXC(I,J,K) = VXC(I,J,K) / VFLD(2,K)
      VYC(I,J,K) = VYC(I,J,K) / VFLD(2,K)
   74 VZC(I,J,K) = VZC(I,J,K) / VFLD(2,K)
C         PRINT OUT MODEL AND CORRECTION VELOCITY RATIOS
      PRINT 2001, (I,(((VX(I,J,K),K=1,25),(VY(I,J,K),K=1,25),(VZ(I,J,
     1K),K=1,25)),J=1,15),I=1,IXLMT)
      PRINT 2001, (I,(((VXC(I,J,K),K=1,25),(VYC(I,J,K),K=1,25),
     1   (VZC(I,J,K),K=1,25)),J=1,15),I=1,IXLMT)
 2001 FORMAT (5(1H1,4H X =  I2// 15(6H V(X)  25F5.2/ 6H V(Y)  25F5.2/
     1  6H V(Z)  25F5.2//)))
C         CORRECT FOR TRANSVERSE VELOCITY COMPONENTS
      DO 80 I = 1,IXLMT
      DO 80 J = 1,IYLMT
      DO 80 K = 1,IZLMT
      VX(I,J,K) = VX(I,J,K) - VXC(I,J,K)
   80 VY(I,J,K) = VY(I,J,K) - VYC(I,J,K)
C         PRINT OUT CORRECTED DATA ARRAYS
      PRINT 2001, (I,(((VX(I,J,K),K=1,25),(VY(I,J,K),K=1,25),(VZ(I,J,
     1K),K=1,25)),J=1,15),I=1,IXLMT)
C         PUNCH OUT CORRECTED DATA ARRAYS
      DO 85 I = 1,IXLMT
      DO 85 J = 1,IYLMT
      PUNCH 2002, I,J,NA1,(K,VX(I,J,K),K= 1, 7)
      PUNCH 2002, I,J,NA1,(K,VX(I,J,K),K= 8,13)
      PUNCH 2002, I,J,NA1,(K,VX(I,J,K),K=14,19)
      PUNCH 2002, I,J,NA1,(K,VX(I,J,K),K=20,25)
      PUNCH 2002, I,J,NA2,(K,VY(I,J,K),K= 1, 7)
      PUNCH 2002, I,J,NA2,(K,VY(I,J,K),K= 8,13)
      PUNCH 2002, I,J,NA2,(K,VY(I,J,K),K=14,19)
      PUNCH 2002, I,J,NA2,(K,VY(I,J,K),K=20,25)
      PUNCH 2002, I,J,NA3,(K,VZ(I,J,K),K= 1, 7)
      PUNCH 2002, I,J,NA3,(K,VZ(I,J,K),K= 8,13)
      PUNCH 2002, I,J,NA3,(K,VZ(I,J,K),K=14,19)
   85 PUNCH 2002, I,J,NA3,(K,VZ(I,J,K),K=20,25)
 2002 FORMAT (I2,I3,1X,A3,1X,7(I2,F8.5))
      PRINT 2003
 2003 FORMAT (1H1)
      GO TO 9
   90 END

      SUBROUTINE CURFT3 (X1,X2,X3,V1,V2,V3,A1,A2,A3)
C          INTERPOLATION SUBROUTINE TO FIND COEFFICIENTS OF THE EQUATION
C                    V = A1*X**2 + A2*X + A3
      A = (X1*X1*X2 + X2*X2*X3 + X3*X3*X1) - (X3*X3*X2 + X2*X2*X1 +
     1   X1*X1*X3)
      B = -((V1*X2 + V2*X3 + V3*X1) - (V3*X2 + V2*X1 + V1*X3))
```

```
      C = (V1*X2*X2 + V2*X3*X3 + V3*X1*X1) - (V3*X2*X2 + V2*X1*X1 +
     1  V1*X3*X3)
      D = -((V1*X2*X2*X3 + V2*X3*X3*X1 + V3*X1*X1*X2) -
     1  (V3*X2*X2*X1 + V2*X1*X1*X3 + V1*X3*X3*X2))
      A1 = -B/A
      A2 = -C/A
      A3 = -D/A
      END
```

```
      PROGRAM CORRECT2

C         PROGRAM TO CORRECT FOR TUNNEL WALL INFLUENCE
      DIMENSION IZ(7), DATA(7), V1(4,15,25), V2(4,15,25), V3(4,15,25),
     1  VRX(4,15,25), VRY(4,15,25), VRZ(4,15,25)
      NA1 = 4HVRX1
      NA2 = 4HVRY2
      NA3 = 4HVRZ3
      NB = 0
   10 DO 11 I = 1,4
      DO 11 J = 1,15
      DO 11 K = 1,25
   11 VRX(I,J,K) = VRY(I,J,K) = VRZ(I,J,K) = 0.0
C         RETURN HERE FOR NEXT GROUP OF DATA
   12 DO 13 I = 1,4
      DO 13 J = 1,15
      DO 13 K = 1,25
   13 V1(I,J,K) = V2(I,J,K) = V3(I,J,K) = 0.0
      N = 1
C         READ IN VELOCITY RATIOS FROM PROGRAM CORRECT1
   20 READ 1000, IX,IY,IDR,(IZ(I),DATA(I),I=1,7)
 1000 FORMAT (I2,I3,3X,I1,1X,7(I2,F8.5))
C         IF EOF GO TO PRINT AND PUNCH SEQUENCE AND PROGRAM END
      IF (EOF,60) 70,21
C         SORT INPUT DATA
   21 GO TO (22,31,41) N
   22 IF (IX-8) 23,23,30
   23 DO 25 I = 1,7
      IF (IZ(I)) 25,25,24
   24 V1(IX,IY,IZ(I)) = DATA(I)
   25 CONTINUE
      GO TO 20
   30 N = 2
      GO TO 20
   31 IF (IX-8) 32,32,40
   32 DO 34 I = 1,7
      IF (IZ(I)) 34,34,33
   33 V2(IX,IY,IZ(I)) = DATA(I)
   34 CONTINUE
      GO TO 20
   40 N = 3
      GO TO 20
   41 IF(IX-8) 42,42,50
   42 DO 44 I = 1,7
      IF (IZ(I)) 44,44,43
   43 V3(IX,IY,IZ(I)) = DATA(I)
   44 CONTINUE
      GO TO 20
C         SET NB = 1 FOR VX, = 2 FOR VY, = 3 FOR VZ
   50 NB = NB + 1
C         CALL SUBROUTINE TO FIND VEL RATIO AT ZERO MODEL SCALE
      DO 58 I = 1,4
      DO 58 J = 1,15
      DO 58 K = 1,25
      GO TO (51,52,52,52,53) J-7
   51 CALL VRAY3 (V1(I,J,K),V2(I,J,K),V3(I,J,K),V)
      GO TO 54
   52 CALL VRAY2 (V1(I,J,K),V2(I,J,K),V)
      GO TO 54
   53 V = V1(I,J,K)
C         PLACE VELOCITY RATIO IN CORRECT ARRAY
```

```
   54 GO TO (55,56,57) NB
   55 VRX(I,J,K) = V
      GO TO 58
   56 VRY(I,J,K) = V
      GO TO 58
   57 VRZ(I,J,K) = V
   58 CONTINUE
C        GO TO PROCESS ANOTHER BATCH OF DATA
      GO TO 12
C        AT EOF COME HERE FOR PRINT AND PUNCH OUT
   70 PRINT 2000, (I,(((VRX(I,J,K),K=1,13),(VRY(I,J,K),K=1,13),
     1  (VRZ(I,J,K),K=1,13)),J=1,15),I=1,4)
 2000 FORMAT (4(1H1,4H X =  I2//15(6H VRX  13F10.5/6H VRY  13F10.5/
     1  6H VRZ  13F10.5//)))
      PRINT 2001,(I,(((VRX(I,J,K),K=14,25),(VRY(I,J,K),K=14,25),
     1  (VRZ(I,J,K),K=14,25)),J=1,15),I=1,4)
 2001 FORMAT (4(1H1,4H X =  I2//15(6H VRX  12F10.5/6H VRY  12F10.5/
     1  6H VRZ  12F10.5//)))
      PRINT 2002, (((VRX(I,J,K),K=1,13),J=1,15),((VRX(I,J,K),K=14,25),
     1    J=1,15),I=1,4)
      PRINT 2002, (((VRY(I,J,K),K=1,13),J=1,15),((VRY(I,J,K),K=14,25),
     1    J=1,15),I=1,4)
      PRINT 2002, (((VRZ(I,J,K),K=1,13),J=1,15),((VRZ(I,J,K),K=14,25),
     1    J=1,15),I=1,4)
 2002 FORMAT (4(1H1,/15(1X,13F10.3/) ///// 15(10X,12F10.3/)))
      DO 60 I = 1,4
      DO 60 J = 1,15
      PUNCH 2004, I,J,NA1,(K,VRX(I,J,K),K= 1, 7)
      PUNCH 2004, I,J,NA1,(K,VRX(I,J,K),K= 8,13)
      PUNCH 2004, I,J,NA1,(K,VRX(I,J,K),K=14,19)
      PUNCH 2004, I,J,NA1,(K,VRX(I,J,K),K=20,25)
      PUNCH 2004, I,J,NA2,(K,VRY(I,J,K),K= 1, 7)
      PUNCH 2004, I,J,NA2,(K,VRY(I,J,K),K= 8,13)
      PUNCH 2004, I,J,NA2,(K,VRY(I,J,K),K=14,19)
      PUNCH 2004, I,J,NA2,(K,VRY(I,J,K),K=20,25)
      PUNCH 2004, I,J,NA3,(K,VRZ(I,J,K),K= 1, 7)
      PUNCH 2004, I,J,NA3,(K,VRZ(I,J,K),K= 8,13)
      PUNCH 2004, I,J,NA3,(K,VRZ(I,J,K),K=14,19)
   60 PUNCH 2004, I,J,NA3,(K,VRZ(I,J,K),K=20,25)
 2004 FORMAT (I2,I3,A4,1X,7(I2,F8.4))
      PRINT 2005
 2005 FORMAT (1H1)
      END

      SUBROUTINE VRAY3 (V1,V2,V3,V)
C        SUBROUTINE TO FIND VEL RATIO AT ZERO MODEL SCALE
C        FROM 3 DATA POINTS
      X1 = .227
      X2 = .490
      X3 = .704
      A = (X1*X1*X2 + X2*X2*X3 + X3*X3*X1) -
     1         (X3*X3*X2 + X2*X2*X1 + X1*X1*X3)
      B = -((V1*X2 + V2*X3 + V3*X1) - (V3*X2 + V2*X1 + V1*X3))
      C = (V1*X2*X2 + V2*X3*X3 + V3*X1*X1) -
     1         (V3*X2*X2 + V2*X1*X1 + V1*X3*X3)
      D = -((V1*X2*X2*X3 + V2*X3*X3*X1 + V3*X1*X1*X2) -
     1         (V3*X2*X2*X1 + V2*X1*X1*X3 + V1*X3*X3*X2))
      V = -D/A
      END
```

```
      SUBROUTINE VRAY2 (V1,V2,V)
C        SUBROUTINE TO FIND VEL RATIO AT ZERO MODEL SCALE
C        FROM 2 DATA POINTS
      X1 = .227
      X2 = .490
      A = X1 - X2
      B = -(V1 - V2)
      C = (V1*X2) - (V2*X1)
      V = -C/A
      END
```

```
      PROGRAM DROPPATH

C         AN ITERATION PROGRAM TO SIMULATE DROPS FALLING THRU A FLOW
C         FIELD AND TO DETERMINE THE PORTION OF DROPS CAUGHT BY THE GAGE
      DIMENSION VX(7,16,25), VY(7,16,25), VZ(7,16,25), IDATA(15)
C         ARRAY USES ARE -
C         VX,VY,VZ - STORAGE OF FIELD DATA COMPONENTS
C         IDATA - TEMP STORAGE OF FIELD DATA
      COMMON /D/NEWDS,NTOT,NHIT
      TYPE REAL MASS
      NEWDS = 1
      NTOT = NHIT = 0
      DO 10 I = 1,7
      DO 10 J = 1,16
      DO 10 K = 1,25
   10 VX(I,J,K) = VY(I,J,K) = VZ(I,J,K) = 0.0
C         READ IN VELOCITY RATIO FIELD DATA
   20 READ 100, IA,IC,IX,IY,(IDATA(I),I=1,15)
  100 FORMAT (3I1,I2,15I5)
      IF (IA .GT. 5) 39,21
C         SORT DATA AND STORE IN PROPER ARRAYS
   21 GO TO (22,27,32) IA
   22 GO TO (23,25) IC
   23 DO 24 I = 1,15
   24 VX(IX+3,IY,I) = IDATA(I)/100.0
      GO TO 20
   25 DO 26 I = 1,10
   26 VX(IX+3,IY,I+15) = IDATA(I)/100.0
      GO TO 20
   27 GO TO (28,30) IC
   28 DO 29 I = 1,15
   29 VY(IX+3,IY,I) = IDATA(I)/100.0
      GO TO 20
   30 DO 31 I = 1,10
   31 VY(IX+3,IY,I+15) = IDATA(I)/100.0
      GO TO 20
   32 GO TO (33,35) IC
   33 DO 34 I = 1,15
   34 VZ(IX+3,IY,I) = IDATA(I)/100.0
      GO TO 20
   35 DO 36 I = 1,10
   36 VZ(IX+3,IY,I+15) = IDATA(I)/100.0
      GO TO 20
C         EXPAND FIELD DATA ARRAYS TO PROVIDE REFLECTED IMAGE OF FLOW
C         FIELD ABOUT THE VERTICAL CENTER PLANE
   39 DO 40 I = 1,3
      DO 40 J = 1,15
      DO 40 K = 1,25
      VX(I,J,K) = -VX(8-I,J,K)
      VY(I,J,K) =  VY(8-I,J,K)
   40 VZ(I,J,K) =  VZ(8-I,J,K)
      DO 41 I = 1,7
      DO 41 J = 1,25
      VX(I,16,J) = VX(I,15,J)
      VY(I,16,J) = VY(I,15,J)
   41 VZ(I,16,J) = VZ(I,15,J)
C         CHECK PRINT OUT OF FIELD DATA
      PRINT 200, (((VX(I,J,K),K=1,25),J=1,15),I=1,7)
      PRINT 200, (((VY(I,J,K),K=1,25),J=1,15),I=1,7)
      PRINT 200, (((VZ(I,J,K),K=1,25),J=1,15),I=1,7)
  200 FORMAT (7(1H1////15(5X,25F5.2//)))
```

```
      PRINT 204
  204 FORMAT (1H1)
      C1 = 4.0*980.1*(0.99820-0.00119)/(3.0*0.00119)
      C2 = 0.001195*3.14159/8.0
      C3 = 3.14159*0.9982/6.0
      G = -980.1
      DT = 0.002
      DX = DZ = 0.25
C         READ IN DROP CHARACTERISTICS
   50 READ 101, DIA,VDT,VF
  101 FORMAT (3F10.2)
      IF (EOF,60) 90,51
C         DETERMINE LIMITS OF DROP STARTING POINTS
   51 XB = XI = 2.0
      XE = 6.0
      YB = YI = 14.5
      ZB = ZI = 14.0*VF/VDT - 2.0
      ZE = ZB + 10.0
      USEYS = -1.0
      IF (ZE .GT. 23.5) 52,55
   52 IF (ZB .GT. 23.5) 53,54
   53 YB = YI = 14.5 - (ZB-23.5)*VDT/VF
      ZB = ZI = 23.5
   54 YE = 14.5 - (ZE-23.5)*VDT/VF
      DY = -DZ*VDT/VF
      USEYS = 1.0
      PRINT 203, YB,YE,DY,ZB,ZE
  203 FORMAT (/8H DP203 * ,5X,3E10.2,5X,2E10.2/)
   55 CONTINUE
      CD = C1*DIA/VDT**2
      MASS = C3*DIA**3
      GM = MASS*G
      X = XB
      Y = YB
      Z = ZB
      C4 = C2*CD*DIA*DIA
      C5 = DT/MASS
      C6 = DT/(2.0*5.08)
C         FIND INITIAL DROP VELOCITIES
   56 VDX = VF*ENT(VX,XI,YI,ZI)
      VDY = VF*ENT(VY,XI,YI,ZI) - VDT
      VDZ = VF*ENT(VZ,XI,YI,ZI)
      PRINT 201, X,Y,Z,VDX,VDY,VDZ,DIA,VF,VDT,CD,ZB,ZE
  201 FORMAT (7H DP201  ,4(2X,3E10.2))
C         FIND NEXT POSITION OF DROP
   60 VFX = VF*ENT(VX,X,Y,Z)
      VFY = VF*ENT(VY,X,Y,Z)
      VFZ = VF*ENT(VZ,X,Y,Z)
      VREL = SQRTF((VFX-VDX)**2+(VFY-VDY)**2+(VFZ-VDZ)**2)
      FD = C4*VREL*VREL
      C7 = C5*FD/VREL
      VDXN = VDX + C7*(VFX-VDX)
      VDYN = VDY + C5*(FD*(VFY-VDY)/VREL+GM)
      VDZN = VDZ + C7*(VFZ-VDZ)
      X = X + C6*(VDXN+VDX)
      Y = Y + C6*(VDYN+VDY)
      Z = Z + C6*(VDZN+VDZ)
      VDX = VDXN
      VDY = VDYN
      VDZ = VDZN
      PRINT 202, X,Y,Z,VDX,VDY,VDZ,XI,ZI,DIA,VF,VDT
  202 FORMAT ( 8H DP202  ,2(5X,3E10.2),5X,2E10.2,2X,3E10.2)
```

```
C         DETERMINE IF DROP HAS REACHED FIELD LIMITS OR CATCH AREA
      IF (Z .LT. 1.) GO TO 74
      IF (X .GT. 6.1 .OR. X .LT. 1.9) GO TO 74
      IF (Y .GT. 2.25) GO TO 60
      CIR = SQRTF(ABSF(4.-(X-4.)**2))
      IF (Y .LT. 1.5 .AND. Z .GE. CIR+3.) GO TO 74
      IF (Y .LT. 1.5 .AND. Z .LE. 3.-CIR) GO TO 74
      IF (Y.LE.2.25 .AND. Z.LE.CIR+3. .AND. Z.GE.3.-CIR) 71,60
   71 IF (CATCH(X,Y,Z) .GT. .5) 72,60
   72 IF (Y-1.5 .LT. (CIR+Z-3.)*VDY/VDZ) 73,74
   73 CALL TALY(X,Y,Z,XI,YI,ZI,DIA,VF,1.)
      GO TO 80
   74 CALL TALY(X,Y,Z,XI,YI,ZI,DIA,VF,0.)
   80 IF (XI .GE. XE) 82,81
   81 X = XI = XI + DX
      Y = YI
      Z = ZI
      GO TO 56
   82 IF (USEYS) 83,83,85
   83 X = XI = XB
      Y = YI
      Z = ZI = ZI + DZ
      IF (ZI .GT. ZE) 84,56
   84 NEWDS = 0
      CALL TALY(X,Y,Z,XI,YI,ZI,DIA,VF,0.)
      GO TO 50
   85 IF (ZI .GE. 23.5) 86,83
   86 X = XI = XB
      Y = YI = YI + DY
      Z = ZI = 23.5
      IF (YI .LT. YE) 84,56
   90 END

      SUBROUTINE TALY(X,Y,Z,XI,YI,ZI,DIA,VF,HM)
C         COUNT DROPS INTERCEPTED AND TOTAL NUMBER FALLEN, PRINT OUT
C         COLLECTED DATA WHEN NEW DROP DATA CARD IS READ
      COMMON /D/NEWDS,NTOT,NHIT
      IF (NEWDS) 10,10,20
   10 HIT = NHIT
      PRO = HIT/(.64*3.14159)
      PRINT 200, NTOT,NHIT,PRO,DIA,VF
  200 FORMAT (/5X,14HTOTAL DROPS = I5,18H, NUMBER CAUGHT = I5,18H, PERCE
     1NT CATCH = F8.2,13H, DROP DIA = F5.3,21HCM, FIELD VELOCITY =
     2F10.1,7H CM/SEC // 1H1)
      NEWDS = 1
      NHIT = NTOT = 0
      RETURN
   20 IF (HM) 22,22,21
   21 NHIT = NHIT + 1
   22 NTOT = NTOT + 1
      PRINT 201, X,Y,Z,DIA,VF,HM,XI,YI,ZI,NHIT,NTOT
  201 FORMAT (  8H TY201   ,13X,2(3E10.2,5X),3E10.2,2I5/)
      RETURN
      END

      FUNCTION CATCH(X,Y,Z)
C         FIND IF DROP HAS ENTERED CATCH FIELD
      IF (Z.GE.2.5.AND.Z.LE.3.5.AND.X.GE.2.5.AND.X.LE.5.5) 50,21
   21 IF (Z.GT.3.5.AND.Z.LE.4..AND.X.GE.3..AND.X.LE.5.) 50,22
   22 IF (Z.LT.2.5.AND.X.LE.Z+3..AND.X.GE.5.-Z) 50,23
   23 IF (Z.GT.4..AND.X.LE.5..AND.X.GE.3..AND.Y.LT.1.5+.75*(5.-Z))50,24
   24 IF (X.LT.4.) GO TO 32
```

```
      IF (Z.LT.2.5) GO TO 28
      IF (Z.GT.3.5.AND.Z.LE.9.-X) 50,25
   25 IF (X.LE.5.5.AND.Y.LT..75*(12.-X-Z)) 50,26
   26 IF (Z.GE.3.5.AND.Y.LT..75*(17.5-2.*X-Z)) 50,27
   27 IF (Y.LT.1.5*(7.-X)) 50,45
   28 IF (Z.GE.X-3.5.AND.X.LE.5.5.AND.Y.LT..5*(7.5+Z-X)) 50,29
   29 IF (X.LE.5.5.AND.Y.LT.2.) 50,30
   30 IF (Z.LE.X-3.5.AND.Y.LE.7.5-X) 50,31
   31 IF (Y.LT.9.25-1.5*X+.5*Z) 50,45
   32 IF (Z.LT.2.5) GO TO 36
      IF (Z.GT.3.5.AND.Z.LE.1.+X) 50,33
   33 IF (X.GE.2.5.AND.Y.LT.3.+.75*(X-Z)) 50,34
   34 IF (Z.GE.3.5.AND.Y.LT.1.125-.75*Z+1.5*X) 50,35
   35 IF (Y.LT.2.25-1.5*(2.5-X)) 50,45
   36 IF (X.GE.2.5.AND.Z.GE.4.5-X.AND.Y.LT..5*(X+Z)-.25) 50,37
   37 IF (X.GE.2.5.AND.Y.LE.2.) 50,38
   38 IF (Z.LE.4.5-X.AND.Y.LE.X-.5) 50,39
   39 IF (Y.LT.1.5*X+.5*Z-2.75) 50,45
   45 CATCH = 0.
      PRINT 101 ,X,Y,Z,CATCH
      RETURN
   50 CATCH = 1.
      PRINT 101 ,X,Y,Z,CATCH
  101 FORMAT ( 8H CAT101  ,5X,3E10.2,5X,E10.2)
      RETURN
      END

      FUNCTION ENT(V,X,Y,Z)
C        INTERPOLATION CONTROL SUBPROGRAM TO FIND VEL RATIO AT (X,Y,Z)
      DIMENSION V(7,16,25),VA(4),VB(4),VC(4)
      XI = IX = X $ YI = IY = Y $ ZI = IZ = Z
      IF (Y .LE. 2.) 50,8
    8 IF (X .LE. 2. .OR. X .GE. 6.) 30,9
    9 IF (Z .LE. 2.) 20,10
   10 DO 17 JZ = 1,4
      DO 16 JX = 1,4
      DO 15 JY = 1,4
   15 VA(JY) = V(IX-2+JX,IY-2+JY,IY-2+JZ)
   16 VB(JX) = ENTD (Y,YI-1.,VA(1),VA(2),VA(3),VA(4))
   17 VC(JZ) = ENTD (X,XI-1.,VB(1),VB(2),VB(3),VB(4))
      ENT = ENTD(Z,ZI-1.,VC(1),VC(2),VC(3),VC(4))
      RETURN
   20 DO 27 JZ = 1,3
      DO 26 JX = 1,4
      DO 25 JY = 1,4
   25 VA(JY) = V(IX-2+JX,IY-2+JY,IZ-1+JZ)
   26 VB(JX) = ENTD(Y,YI-1.,VA(1),VA(2),VA(3),VA(4))
   27 VC(JZ) = ENTD(X,XI-1.,VB(1),VB(2),VB(3),VB(4))
      ENT = ENTC(Z,ZI,VC(1),VC(2),VC(3),0.)
      RETURN
   30 AI = II = 1
      IF (X .LE. 2.) AI = II = 0
      IF (Z .LE. 2.) GO TO 40
      DO 37 JZ = 1,4
      DO 36 JX = 1,3
      DO 35 JY = 1,4
   35 VA(JY) = V(IX-1+JX-II,IY-2+JY,IZ-2+JZ)
   36 VB(JX) = ENTD(Y,YI-1.,VA(1),VA(2),VA(3),VA(4))
   37 VC(JZ) = ENTC(X,XI-AI,VB(1),VB(2),VB(3),0.)
      ENT = ENTD(Z,ZI-1.,VC(1),VC(2),VC(3),VC(4))
      RETURN
   40 DO 47 JZ = 1,3
```

```
      DO 46 JX = 1,3
      DO 45 JY = 1,4
   45 VA(JY) = V(IX-1+JX-II,IY-2+JY,IZ-1+JZ)
   46 VB(JX) = ENTD(Y,YI-1.,VA(1),VA(2),VA(3),VA(4))
   47 VC(JZ) = ENTC(X,XI-AI,VB(1),VB(2),VB(3),0.)
      ENT = ENTC(Z,ZI,VC(1),VC(2),VC(3),0.)
      RETURN
   50 IF (X .LE. 2. .OR. X .GE. 6.) GO TO 70
      IF (Z .LE. 2.) GO TO 60
      DO 57 JZ = 1,4
      DO 56 JX = 1,4
      DO 55 JY = 1,3
   55 VA(JY) = V(IX-2+JX,IY-1+JY,IZ-2+JZ)
   56 VB(JX) = ENTC(Y,YI,VA(1),VA(2),VA(3),0.)
   57 VC(JZ) = ENTD(X,XI-1.,VB(1),VB(2),VB(3),VB(4))
      ENT = ENTD(Z,ZI-1.,VC(1),VC(2),VC(3),VC(4))
      RETURN
   60 DO 67 JZ = 1,3
      DO 66 JX = 1,4
      DO 65 JY = 1,3
   65 VA(JY) = V(IX-2+JX,IY-1+JY,IZ-1+JZ)
   66 VB(JX) = ENTC(Y,YI,VA(1),VA(2),VA(3),0.)
   67 VC(JZ) = ENTD(X,XI-1.,VB(1),VB(2),VB(3),VB(4))
      ENT = ENTC(Z,ZI,VC(1),VC(2),VC(3),0.)
      RETURN
   70 AI = II = 1
      IF (X .LE. 2.) AI = II = 0
      IF (Z .LE. 2.) GO TO 80
      DO 77 JZ = 1,4
      DO 76 JX = 1,3
      DO 75 JY = 1,3
   75 VA(JY) = V(IX-1+JX-II,IY-1+JY,IZ-2+JZ)
   76 VB(JX) = ENTC(Y,YI,VA(1),VA(2),VA(3),0.)
   77 VC(JZ) = ENTC(X,XI-AI,VB(1),VB(2),VB(3),0.)
      ENT = ENTD(Z,ZI-1.,VC(1),VC(2),VC(3),VC(4))
      RETURN
   80 DO 87 JZ = 1,3
      DO 86 JX = 1,3
      DO 85 JY = 1,3
   85 VA(JY) = V(IX-1+JX-II,IY-1+JY,IZ-1+JZ)
   86 VB(JX) = ENTC(Y,YI,VA(1),VA(2),VA(3),0.)
   87 VC(JZ) = ENTC(X,XI-AI,VB(1),VB(2),VB(3),0.)
      ENT = ENTC(Z,ZI,VC(1),VC(2),VC(3),0.)
      RETURN
      END

      FUNCTION ENTD(X,XA,VA,VB,VC,VD)
C        NEWTON INTERPOLATION SCHEME - THIRD ORDER
      A = VB - VA
      B = VC - VB
      XI = X - XA
      ENTD = VA + XI*(A + (XI-1.)*(.5*(B-A)+(XI-2.)*(.5*(VD-VC-B)-
     1   .5*(B-A))/3.))
      RETURN
C        ENTRY POINT FOR SECOND ORDER INTERPOLATION
      ENTRY ENTC
      ENTD = VA + (X-XA)*(VB-VA+(X-XA-1.)*.5*(VC-VB-VB+VA))
      RETURN
      END
```